Isotope paleohydrology and environment of Devonian bivalve fossils from the Weatherall and Hecla Bay formations, Melville Island, Canadian Arctic.

A Thesis Submitted to the College of
Graduate Studies and Research,
in Partial Fulfilment of the Requirements
for the Degree of Master of Science,
in the Department of Geological Sciences,
University of Saskatchewan,
Saskatoon.

By
Rebekah Hines
Fall 2001

PERMISSION TO USE

In presenting this thesis in partial fulfilment of the requirements for a Postgraduate degree from the University of Saskatchewan, I agree that the Libraries of this University may make it freely available for inspection. I further agree that permission for copying of this thesis in any manner, in whole or in part, for scholarly purposes may be granted by the professor or professors who supervised my thesis work or, in their absence, by the Head of the Department or the Dean of the College in which my thesis work was done. It is understood that any copying or publication or use of this thesis or parts thereof for financial gain shall not be allowed without my written permission. It is also understood that due recognition shall be given to me and to the University of Saskatchewan in any scholarly use which may be made of any material in my thesis.

Requests for permission to copy or to make other use of material in this thesis in whole or part should be addressed to:

Head of the Department of Geological Sciences
University of Saskatchewan
114 Science Place
Saskatoon, Saskatchewan
S7N 5E2

ABSTRACT

Sr, O and C isotopic measurements of Devonian bivalves were performed to elucidate the isotope paleohydrology of an unusual bivalve-dominated marginal marine sequence from the siliciclastic Weatherall and Hecla Bay formations of Melville Island.

To confirm that measured isotopic compositions had not been completely overprinted by diagenesis, considerable evidence was amassed indicating that the bivalves had been subjected to relatively closed-system diagenesis. XRD analysis indicated that the fossils contain up to 18 % relic aragonite, finely disseminated on a millimetre scale within the recrystallized shell.

The $^{87}Sr/^{86}Sr$ – Ca/Sr diagram was used to separate potential diagenetic trends from environmental trends. Trend lines defined by individual species from single handsamples were extrapolated toward lower Ca/Sr and lower $^{87}Sr/^{86}Sr$, resulting in convergence of the trend lines within a relatively narrow range of $^{87}Sr/^{86}Sr$ ratios, which is interpreted as the mean $^{87}Sr/^{86}Sr$ range for the depositional waters, averaged over all facies.

Using the $^{87}Sr/^{86}Sr$ ratios and estimates of the $^{87}Sr/^{86}Sr$ and Sr concentration of Devonian marine and freshwaters, Sr material balance calculations yielded paleosalinities between 0 $^{o}/_{oo}$ and 14 $^{o}/_{oo}$ for the bivalves' depositional waters and a 1000 Sr/Ca ratio of 12.5 for Devonian seawater. Oxygen isotope balance calculations yielded paleosalinities between 0 $^{o}/_{oo}$ and 19 $^{o}/_{oo}$. While the paleosalinity ranges determined using these two methods are similar, salinity values calculated for individual species are consistent only in certain specimens of *Limoptera* sp., suggesting evaporative enrichment of ^{18}O in the mixing zone or diagenesis. The calculated $^{87}Sr/^{86}Sr$ salinity values are consistent with sedimentological studies of the area, which suggest a deltaic environment of deposition.

ACKNOWLEDGEMENTS

I am grateful to my supervisors, Dr. C. Holmden and Dr. J. Basinger, and to Dr. P. Johnston for the opportunity to work and study with them, as well as their helpful comments, editing, and support.

Many thanks are extended to D. Fox for instruction in analytical techniques and invaluable advice in the laboratory, N. Sherstyuk and T. Bonli for extensive technical assistance and instruction above and beyond the call of duty, and Dr. Y. Pan for instruction in XRD analysis. The insightful observations and suggestions of Dr. D. De Boer, Dr. D. Milne, and Dr. B. Pratt were greatly appreciated.

The friendship and support of K. Fanton, M. Mathé, K. Panchuk, and D. Wright are gratefully acknowledged, with special thanks to the Queen Mum and Chairman Mao.

I'm extremely grateful to my parents for their ongoing love and support and to K & M for cable, Chinese, and ice cream.

This study was supported by an individual research grant to Dr. C. Holmden from the Natural Sciences and Engineering Research Council of Canada.

TABLE OF CONTENTS

LIST OF TABLES

Table

LIST OF FIGURES

Figure

1.0 INTRODUCTION

Devonian marine fossil assemblages are composed primarily of corals and brachiopods. The studied siliciclastic lithologies of the Weatherall and Hecla Bay formations, although underlain by Devonian siltstone and shale containing normal marine assemblages, contain predominantly mollusk fossils (Johnston & Goodbody, 1988). This bivalve-dominated assemblage is unusual for the Devonian and suggests unusual depositional waters, which may be related to salinity, as the study site is thought to be located at the interface of braided stream and marine environments, in the deltaic zone of mixed waters (Embry & Klovan, 1976; Embry, 1988; Goodbody, 1988; Johnston & Goodbody, 1988; Embry, 1991; Goodbody, 1994).

While sedimentological studies have been quite useful in qualitative study of the deposited lithologies, they do not provide the means for quantification of paleohydrological parameters such as salinity. For this reason, Sr, O and C isotopes will be used to confirm previous interpretations, based on sedimentological information, of the depositional environment of the Weatherall and Hecla Bay formations.

Isotopic reconstruction of the paleohydrology allows evaluation of the range of potential salinity variation in the Weatherall and Hecla Bay depositional waters relative to contemporaneous seawater and freshwater (e.g. Clayton & Degens, 1959; Mook & Vogel, 1967; Dodd & Stanton, 1975; Hudson *et al.*, 1995; Hendry & Kalin, 1997; Andersson *et al.*, 1992; Holmden *et al.*, 1997)

Because marine and fresh waters have greatly contrasting isotopic signatures for 0, C and Sr, it is possible to determine from the isotopic compositions of Melville Island mollusk shells whether they were precipitated in waters controlled by mixing of seawater and freshwater. From this type of paleohydrological analysis, proxy salinities can be resolved and the Devonian paleosalinity regime of central Melville Island elucidated.

2.0 BACKGROUND

2.1 Geological setting and stratigraphy

Situated in the Canadian Arctic Archipelago, Melville Island offers excellent exposure of Devonian clastic shelf and deltaic systems (Figure 2-1) (Goodbody, 1988; 1994). As Devonian paleogeography is the subject of a great diversity of opinion, there are varying interpretations of the geographic location of Melville Island in the Middle Devonian. While a recent study (Scotese, 2000) places Melville Island directly on the equator, some earlier paleogeographic reconstructions place it approximately 12° (Scotese and McKerrow, 1990) to 17° (Ziegler, 1988) North of the equator. This source of variability must be considered when undertaking paleoenvironmental reconstruction. From the Middle Devonian to the Early Carboniferous, the Ellesmerian Orogeny folded and uplifted the Canadian Arctic, resulting in the creation of the Ellesmerian and Caledonian Mountains to the north-east of Melville Island (Goodbody, 1988; 1994; Harrison, 1994) and in the influx of clastic material from these mountains to the study area (Figure 2-2). This deposition of clastic material continued into the Famennian (Embry and Klovan, 1976; Goodbody & Christie; 1994) and resulted in the formation of the Middle Devonian clastic wedge. On Melville Island, the clastic wedge shows a generally regressive pattern, with evident southwesterly migration of facies (Goodbody, 1988).

In the Canadian Arctic, the Middle Devonian clastic wedge is made up of three distinct sediment subwedges, all of which are present on Melville Island: The Hecla Bay, Parr

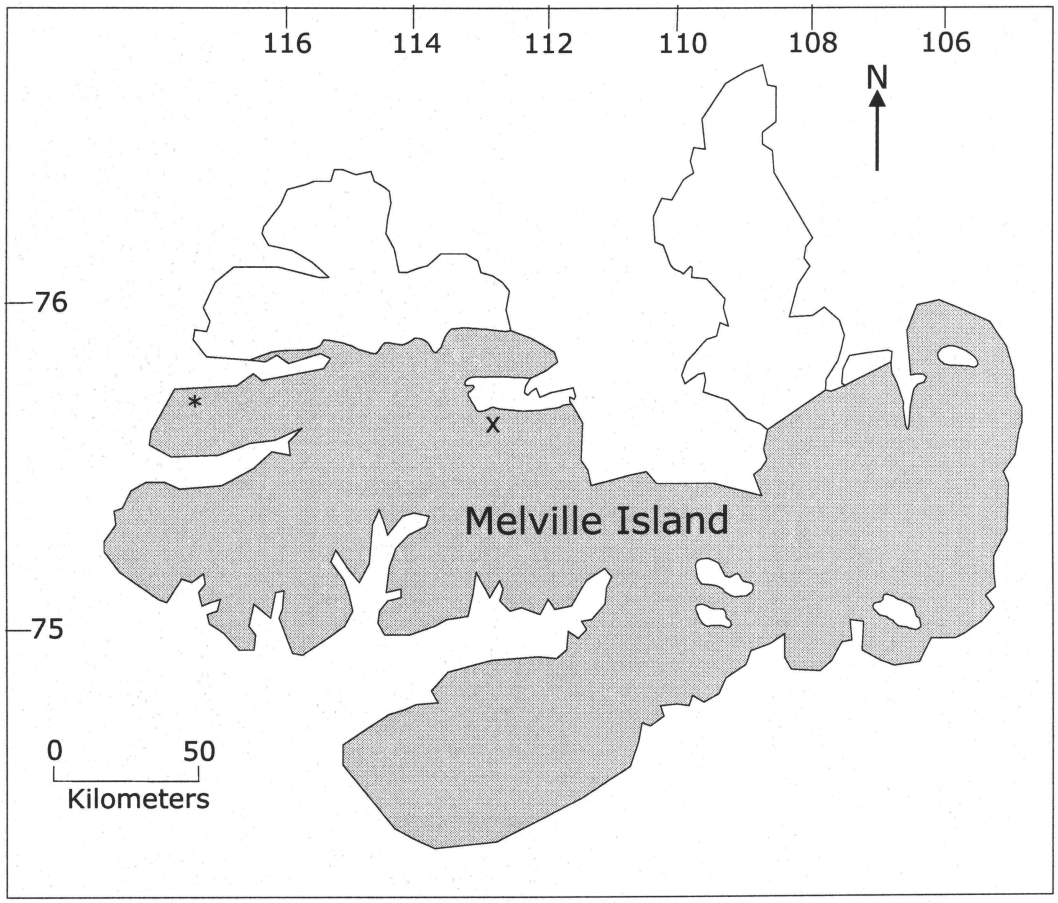

Figure 2-1. Simplified geology of Melville Island (modified from Harrison *et al.*, 1985) showing exposure of the Devonian clastic wedge (shaded), as well as approximate locations of the Ibbett Bay (*) and McCormick Inlet (x) bivalve assemblages.

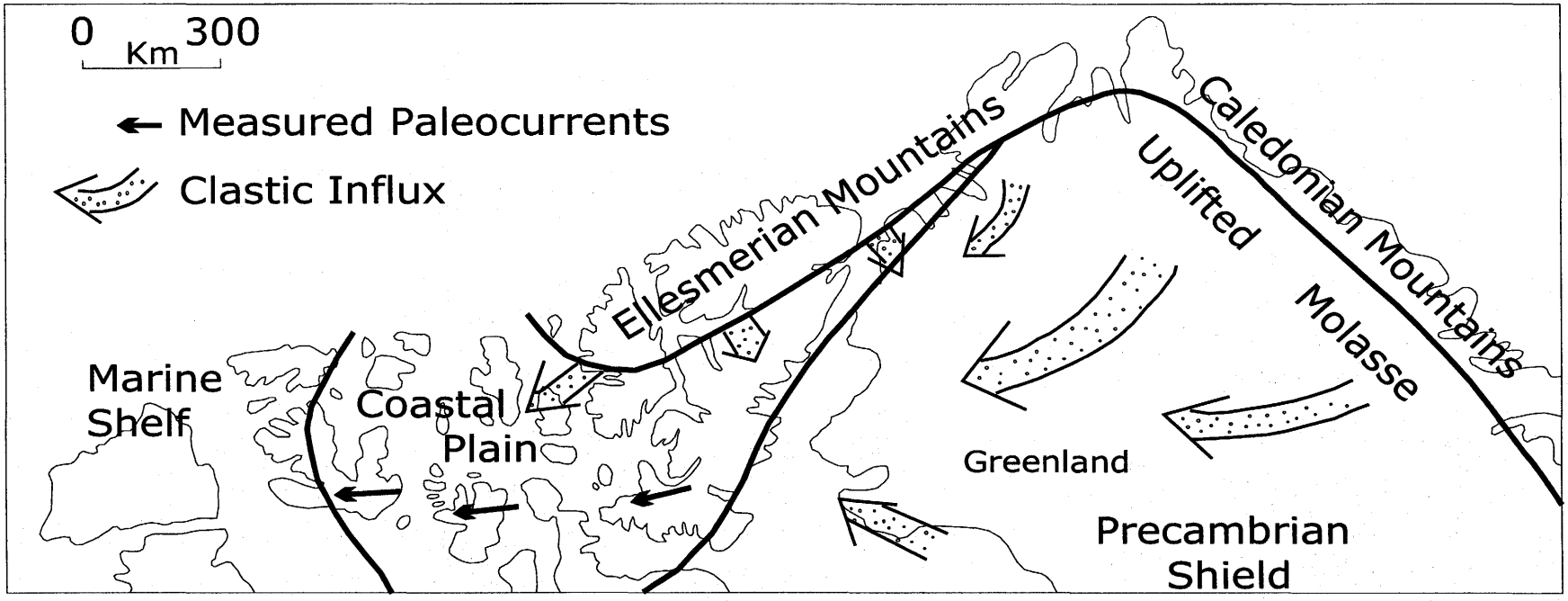

Figure 2-2. Late Givetian paleogeography of the Canadian Arctic Archipelago (from Embry, 1988).

Islands and Beverley Inlet subwedges (Figure 2-3) (e.g. Embry and Klovan, 1976; Goodbody, 1988; Goodbody, 1994; Goodbody & Christie; 1994; Harrison, 1994).

Weatherall Formation - Part of the Hecla Bay subwedge, the Weatherall Formation overlies the outer-shelf to slope deposits of the Cape De Bray Formation (figures 2-3 and 2-4). In eastern Melville Island, the Weatherall Formation is over 1000 m thick and consists of coarsening-upward sequences of shale, siltstone and sandstone (Goodbody, 1988; 1994). Trace fossils, brachiopods, bivalves and trilobites abound (Goodbody, 1988; 1994), indicating a marine environment of deposition. In north-central Melville Island (McCormick Inlet; Figure 2-1), the Weatherall Formation is up to 1500 m thick and has a high shale content (Goodbody, 1988; 1994). Brachiopods are present in the lower portion of the formation, while bivalve and bellerophontid assemblages are more prevalent in the higher portions (Goodbody, 1988; 1994). In western Melville Island (Ibbett Bay; Figure 2-1), the shales, siltstones and silty sandstones of the Weatherall Formation are extensively intercalated with the non-calcareous sandstones of the Hecla Bay Formation. This lithological interdigitation, described by Goodbody (1988) as the Weatherall and Hecla Bay Complex, is interpreted as shelf and deltaic/coastal deposits (e.g. Embry and Klovan, 1976; Goodbody, 1988; 1994).

Hecla Bay Formation - The Hecla Bay Formation overlies the Weatherall Formation and is characterised by fine to medium grained sandstone with siltstones and shales, sandstone being the predominant lithology (Figure 2-1) (Goodbody, 1988; 1994). While it is up to 1050 m thick on the eastern portion of the island, the formation thins to the west (Goodbody, 1988; 1994), resulting in complex interfingering with the Weatherall Formation as described above. There is evident cross-stratification and broad, shallow channels are apparent (Goodbody, 1988). As the sampled areas of the Weatherall and

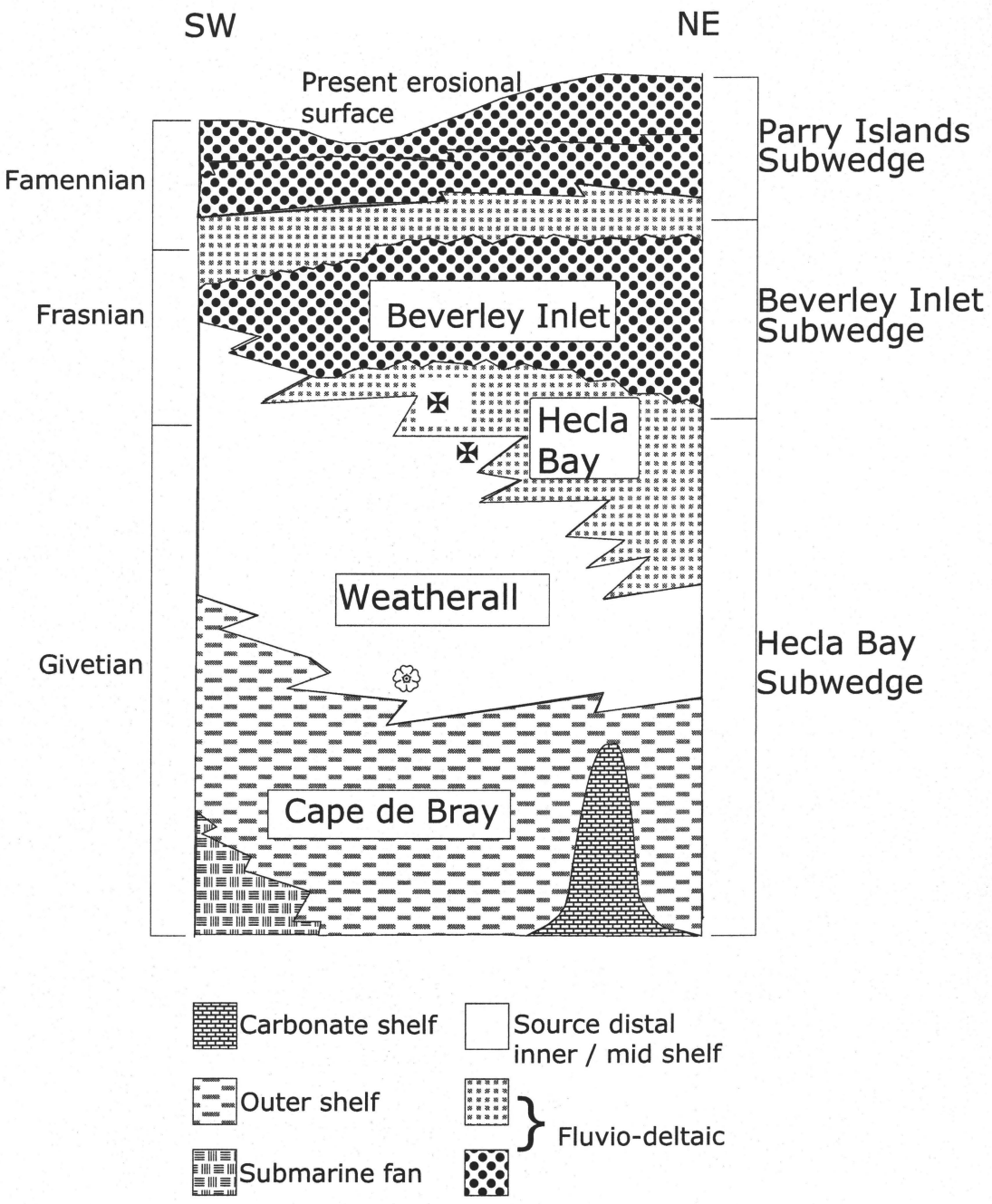

Figure 2-3. Schematic regional cross-section of Melville Island through the Devonian clastic wedge, showing the Hecla Bay, Beverley Inlet and Parry Islands subwedges, as well as the approximate locations of collected bivalve (✠) and brachiopod (❀) specimens (modified after Embry & Klovan, 1976; Embry, 1994; Goodbody, 1994).

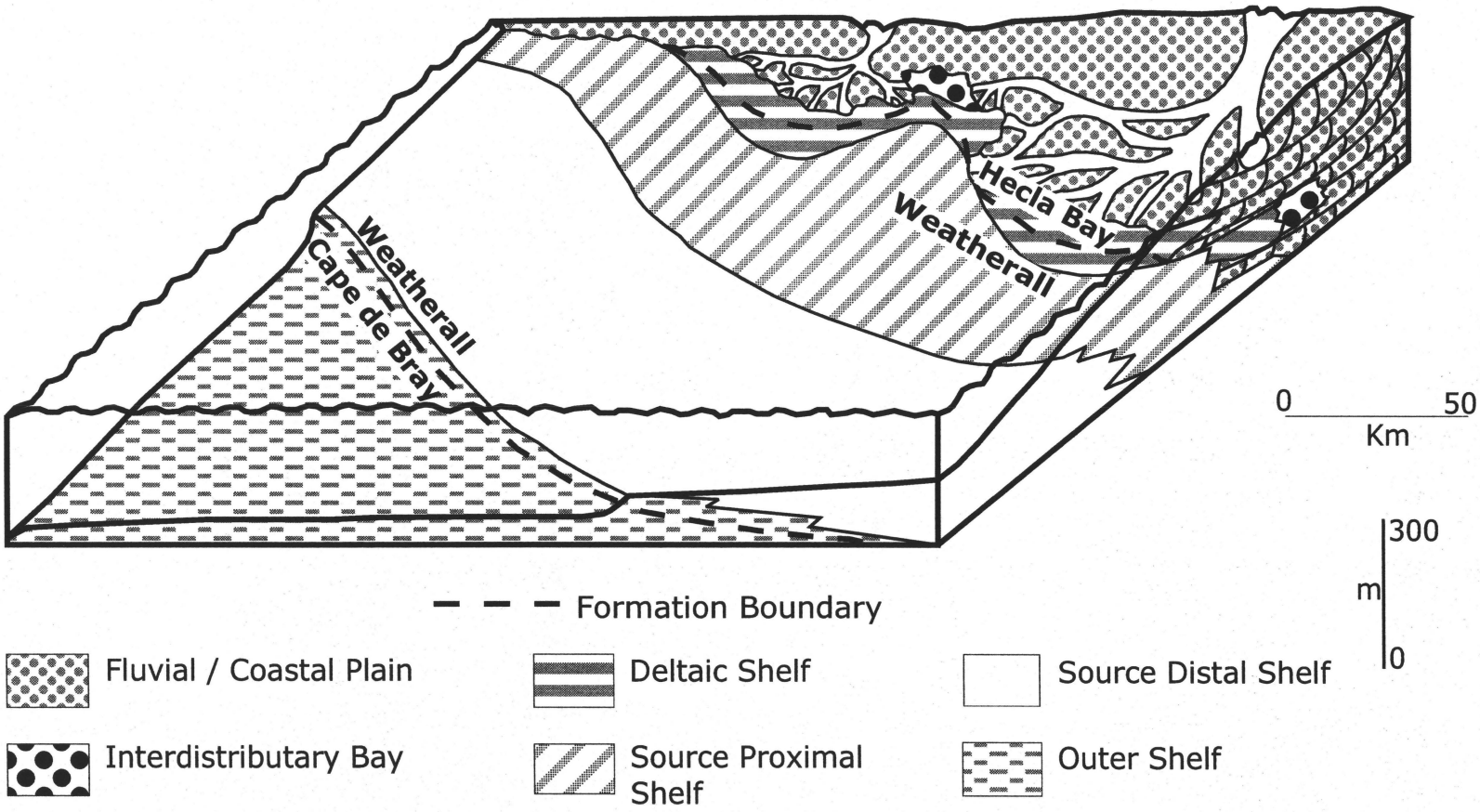

Figure 2-4. Formations, environments of deposition, and their spatial relationships, western Melville Island (modified from Goodbody, 1988).

Hecla Bay Formations (Figure 2-3) are interpreted as being of fluviodeltaic origin (e.g. Embry and Klovan, 1976; Goodbody, 1988; 1994), in order to accurately evaluate the paleohydrology of these formations on Melville Island, the processes governing such deposits must be considered.

The following description of deltas is drawn from the works of Barrell (1912), Coleman (1981) and Nemec (1990).

A delta is defined as a deposit built by riverine flow into a permanent body of standing water (e.g. Barrell, 1912; Nemec, 1990), and regulated by the river system, dynamic processes such as tidal or wave action, and any interaction between the fluvial regime and riverborne sediments (Nemec, 1990).

The river system consists of four principal elements: the drainage basin, the alluvial valley, the deltaic plain and the receiving basin (Coleman, 1981). Of particular importance to this study is the deltaic plain, made up of both subaqueous and subaerial sections. The fraction of the deltaic plain situated below the low tide water level constitutes the subaqueous section (Figure 2-5), while the subaerial region, made up of the upper and lower delta plains (Figure 2-5), is located above the low tide limit and is older than the subaqueous component (Coleman, 1981). In an active delta, which is dynamically prograding and occupied by operative distributary channels (Coleman, 1981), the subaqueous delta plain forms the foundation for sediment progradation and shows a seaward fining of sediment, as evidenced in the Hecla Bay Formation on western Melville Island. The coarsest deposits constitute the distributary mouth bar, which is located a short distance from the river mouth (e.g. Coleman, 1981). Seaward of the distributary mouth bar are found the delta front deposits, a zone of interfingering silts, sands and clays resembling the Weatherall and Hecla Bay Complex at Ibbett Bay.

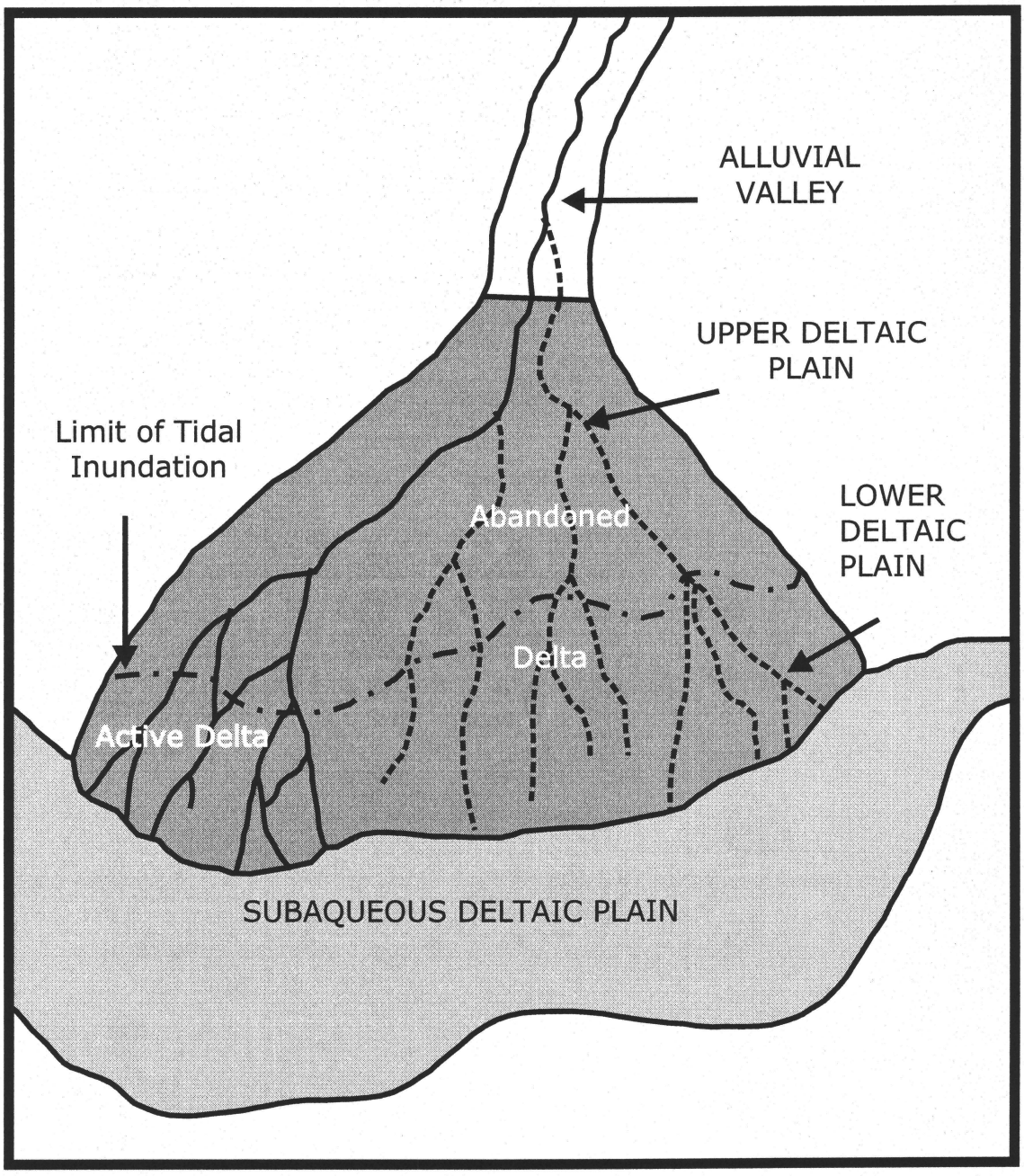

Figure 2-5. Principal elements of the deltaic plain (from Coleman, 1981).

As the system progrades, subaerial deltaic sediments are deposited over the upper subaqueous sediments and, as seen in eastern portions of the Weatherall Formation, a coarsening-upward succession becomes evident over time.

As the density of seawater is much greater than that of freshwater, in a deltaic environment, the freshwater output spreads over the seawater, forming a plane jet (Bates, 1953). This induces a reverse seawater flow underneath, causing the shoreward migration of the seawater layer and resulting in a zone of freshwater - seawater mixing (Bates, 1953). Due to the increased riverine and reduced marine influences on a fluvial dominated delta, the mixing zone can be quite extensive, and brackish waters may occur to a greater depth than in a wave- or tide-dominated deltaic system.

2.2 Samples

Because existing studies of macro-invertebrates from the Devonian of the Canadian Arctic focus on corals and brachiopods, which commonly dominate fossil assemblages, very little is known about bivalves from the Devonian of Melville Island. In addition, as few modern systematic compilations of Devonian bivalve faunas exist, biogeographical interpretation is limited (Johnston & Goodbody, 1988). As a result, the bivalve-dominated assemblages of Melville Island present an exceptional opportunity to study a seldom-analysed brackish water assemblage.

The studied bivalves include *Nuculopsis* sp., *Limoptera* sp., Nyassidae n. gen. & n. sp., Montanariidae n. gen. & n. sp., and *Montanaria* sp. and are evident as both storm lag assemblages, occurring in dense, thin accumulations of disarticulated and fragmented shells, and *in situ* assemblages, which often contain complete articulated shells, at times in presumed life position (Johnston & Goodbody, 1988). While trilobites and brachiopods are rare and often fragmented, the bivalve-dominated assemblages occur in

a variety of lithofacies ranging from deltaic to source-proximal to distal non-deltaic, shallow shelf environments (Figure 2-6) (Goodbody, unpublished data, 1987; Johnston & Goodbody, 1988).

In the Weatherall Formation of McCormick Inlet (Figure 2-1), Montanariidae n. gen. n. sp. is found in the source proximal shelf environment (Figure 2-6) (Goodbody, unpublished data, 1987; Johnston, personal communication, 1998), while Nyassidae n. gen. & n. sp., and *Nuculopsis* sp. are restricted to the source distal area (Figure 2-6). *Limoptera* sp. occurs in a variety of facies, ranging from the top of the clastic shelf rhythm, near the transition to the delta marginal shelf environment at Ibbett Bay, and from the base of the source distal shelf area to the source proximal shelf at McCormick Inlet. *Limoptera* sp. specimens were selected from the source distal shelf environment for analysis (Figure 2-6).

Brachiopods were sampled from the mud-dominated source distal environment of the Weatherall Formation of Ibbett Bay.

In the Hecla Bay Formation of Ibbett Bay (Figure 2-1), *Montanaria* sp., known only from this locality, is evident in great numbers in the interdistributary bay environment (Figure 2-6) (Goodbody, unpublished data, 1987). The fact that this species does not occur in the more distal environments of the Weatherall and Hecla Bay formations, as well as its relative stratigraphic position, suggests conditions of reduced salinity (Johnston, personal communication, 2001). In addition, while the presence of *Trypanites* borings in some specimens indicates some marine influence, only 5% of specimens contain such borings, which are sparsely distributed and small, suggesting the larvae were unable to successfully establish themselves, probably as a result of reduced marine influence (Johnston, personal communication, 2001). There is also a shell bed,

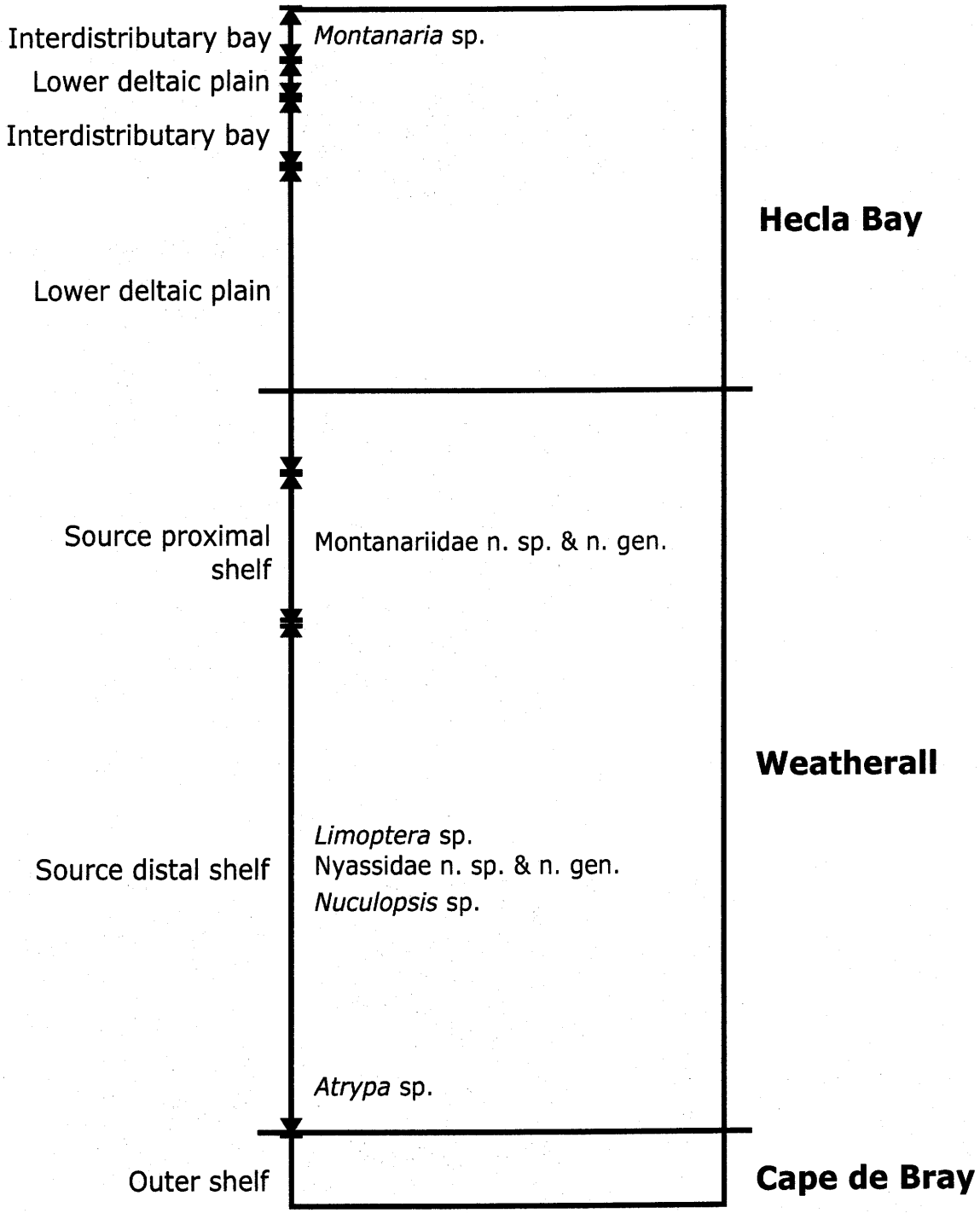

Figure 2-6. Schematic stratigraphic column showing vertical facies relationships and approximate locations of sampled species.

composed entirely of *Montanaria* sp., up-section from all other specimens used in this study. This monospecific shell bed is further indication of an unusual depositional environment, possibly related to paleosalinity.

Many species that dominate modern brackish water environments, such as the deltaic mixing zone, are also evident in other marine milieus (Barnes, 1989). In fact, while species diversity studies show that a minimal number of species are found in the 5 $^{o}/_{oo}$ to 8 $^{o}/_{oo}$ salinity range, in most modern brackish water environments, the species present constitute a subset of adjacent marine communities (Barnes, 1989). Therefore, the degree to which it is possible to interpret the paleoenvironment, notably the paleosalinity regime, based solely on the physiological characteristics of an assemblage of fossil material is questionable (Barnes, 1989). For this reason, this study will employ isotope geochemistry to further define the paleosalinity regime of the Middle Devonian of Melville Island.

2.3 Isotope systems

Marine and fresh waters have generally contrasting isotopic compositions for O, C and Sr (e.g. Andersson *et al.*, 1992; Ingram and DePaolo, 1993; Holmden *et al.*, 1997). Because of such contrasts in isotopic composition, it is possible to determine from the isotopic compositions of Melville Island mollusk shells whether they were precipitated in waters controlled by mixing of seawater and freshwater. From this type of paleohydrological analysis, proxy salinities can be determined.

2.3.1 Oxygen

The $\delta^{18}O$ content of shell carbonate material is dependent on the temperature and isotopic composition of the water in which it was precipitated. Assuming minimal

temperature variation between marine and freshwater endmembers, changes in $\delta^{18}O_{shell}$ values precipitated from brackish waters should reflect differences in salinity between these endmembers, assuming conservative two-component mixing (Dodd & Stanton, 1975; Hudson *et al.*, 1995; Holmden *et al.*, 1997). Conservative two-component mixing implies that the salinity of brackish water is controlled solely by dilution of seawater by riverine water. For example: Given a seawater endmember with a salinity of 35 $^{o}/_{oo}$ and a freshwater endmember with a salinity of 0 $^{o}/_{oo}$, mixing of equal volumes of the two waters, would yield a salinity of 17.5 $^{o}/_{oo}$. $\delta^{18}O$ data from mollusk shells precipitated in a brackish water environment (such as is suggested for the study area) can be used to plot a linear seawater - freshwater mixing line as $\delta^{18}O$ provides a proxy record of salinity according to

$$\delta^{18}O_{mix} = \delta^{18}O_{seawater}\,\chi + \delta^{18}O_{freshwater}\,(1-\chi) \qquad (2.1)$$

where χ is the fraction of seawater in the mixture.

There are, however, drawbacks to this method (Holmden *et al.*, 1997; Hendry *et al.*, 1997), in that the ^{18}O content of water is directly affected by evaporation; as ^{16}O is the lighter isotope, $H_2{}^{16}O$ will evaporate faster than $H_2{}^{18}O$, and the remaining water will therefore be ^{18}O enriched. Thus, if a body of brackish water has a very slow mixing rate between marine and fresh waters (long residence time), shell $\delta^{18}O$ values may be higher than predicted by two-component mixing between marine and fresh waters. The assumption of two-component conservative mixing would, therefore, not be valid if extensive evaporation had occurred in the mixing zone, and the salinities calculated would be too high.

2.3.2 Carbon

In marine environments, $\delta^{13}C$ values for dissolved inorganic carbon (DIC) are around 0 $^{o}/_{oo}$ while freshwater DIC is generally more ^{13}C depleted, resulting in $\delta^{13}C$ values as low as -30 $^{o}/_{oo}$ PDB (Pee Dee Belemnite) (Craig, 1961). One might therefore expect to be able to construct a two-component mixing curve using $\delta^{13}C$ values from brackish water mollusk shells, assuming conservative two-component mixing of marine and riverine sources (Mook, 1970). However, the aforementioned hypothesis can be easily compromised by a number of processes operating in the seawater-freshwater mixing zone that influence the isotopic composition of dissolved inorganic carbon; the DIC in paleowaters is subject to CO_2 exchange between atmosphere and water (net uptake of ^{13}C), local production of ^{13}C depleted, metabolically derived CO_2, photosynthetic activity of local aquatic flora (uptake of ^{12}C), oxidation of organic matter (release of ^{12}C), as well as local weathering of marine limestones (release of ^{13}C).

2.3.3 Strontium

There is no isotope effect on Sr partitioning into shell carbonate due to temperature variation, or from evaporation of the depositional waters. As a result, Sr isotopes in fossil shells directly record the Sr isotopic composition of the habitat waters. They will therefore be employed as an additional method of determining the degree of seawater - freshwater mixing, and thus the paleosalinity, of the studied depositional environment. If the $^{87}Sr/^{86}Sr$ ratios and Sr concentrations of contemporaneous marine and riverine endmembers are known, one can construct two-component mixing curves. These define hyperbolae, where the degree of curvature is a function of the mixing endmembers' concentrations and isotopic abundances. By determining the hyperbolic mixing curve of

a specific hydrological region, proxy salinities can be calculated for $^{87}Sr/^{86}Sr$ ratios assumed to result from mixing of marine and freshwaters (Holmden *et al.*, 1997). Using the modern ocean Sr concentration of 7.7 ppm, for example, and given that a $^{87}Sr/^{86}Sr$ ratio of 0.7079 is characteristic for seawater in the Devonian (Veizer *et al.*, 1999), while a $^{87}Sr/^{86}Sr$ ratio of 0.7119 and a Sr concentration of 0.071 ppm are characteristic of rivers (Holmden, 1997), one can construct a theoretical hyperbolic mixing curve for Melville Island in the Devonian (Figure 2-7). Salinity values can then be calculated using the expression

$$\frac{S_{BW}}{35^{o}/_{oo}} = \frac{Sr_{FW}\left(\frac{^{87}Sr}{^{86}Sr}\right)_{FW} - Sr_{FW}\left(\frac{^{87}Sr}{^{86}Sr}\right)_{BW}}{\left(\frac{^{87}Sr}{^{86}Sr}\right)_{BW}(Sr_{SW} - Sr_{FW}) - \left[Sr_{SW}\left(\frac{^{87}Sr}{^{86}Sr}\right)_{SW} - Sr_{FW}\left(\frac{^{87}Sr}{^{86}Sr}\right)_{FW}\right]} \qquad (2.2)$$

where FW and SW refer to the freshwater and seawater endmembers, respectively, and S_{BW} is the salinity of the brackish body of water.

Due to the hyperbolic nature of this mixing curve, there is systematic variation in the uncertainty of paleosalinity determinations, which increases with salinity. As a constant Sr concentration is assumed for seawater, which has a uniform $^{87}Sr/^{86}Sr$ (Holmden, *et al.*, 1997), the shape of the mixing curve and, consequently, the range of precise paleosalinity determination, are controlled by the $^{87}Sr/^{86}Sr$ ratio and Sr concentration of freshwater. Due to the analytical uncertainty of ± 0.00002 on the $^{87}Sr/^{86}Sr$ ratio, high precision salinity calculations are most resolvable over the area of greatest curvature, between $^{87}Sr/^{86}Sr$ ratios of 0.7119 and 0.7085 (Figure 2-8). Because the most precise paleosalinity values are resolved from the low-salinity end of the spectrum, there is a

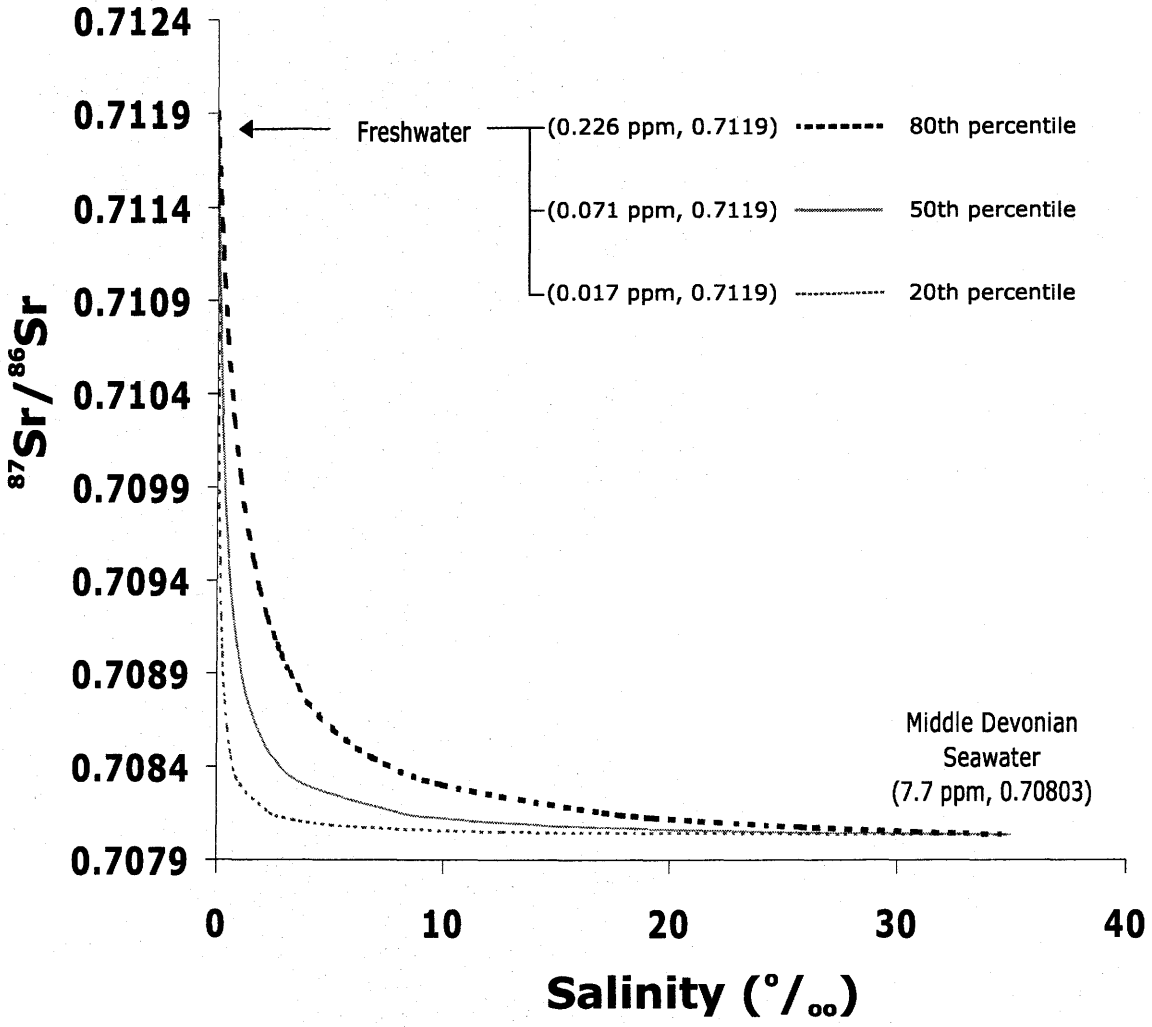

Figure 2-7. Two-component mixing curves for the Middle Devonian of Melville Island based on $^{87}Sr/^{86}Sr$ paleohydrology. The $^{87}Sr/^{86}Sr$ freshwater endmember is determined using mean world river data from Holmden *et al.* (1997). The $^{87}Sr/^{86}Sr$ seawater endmember is determined using *Atrypa* sp. (TMP# 1987.174.2) from the base of the Weatherall Formation, this study. The solid curve is constructed with these seawater and freshwater endmembers and the median (50^{th} percentile) values for the Sr concentration of freshwater in world rivers and lakes. The dashed curves are plotted using 20^{th} and 80^{th} percentile values, respectively, for Sr concentration in rivers.

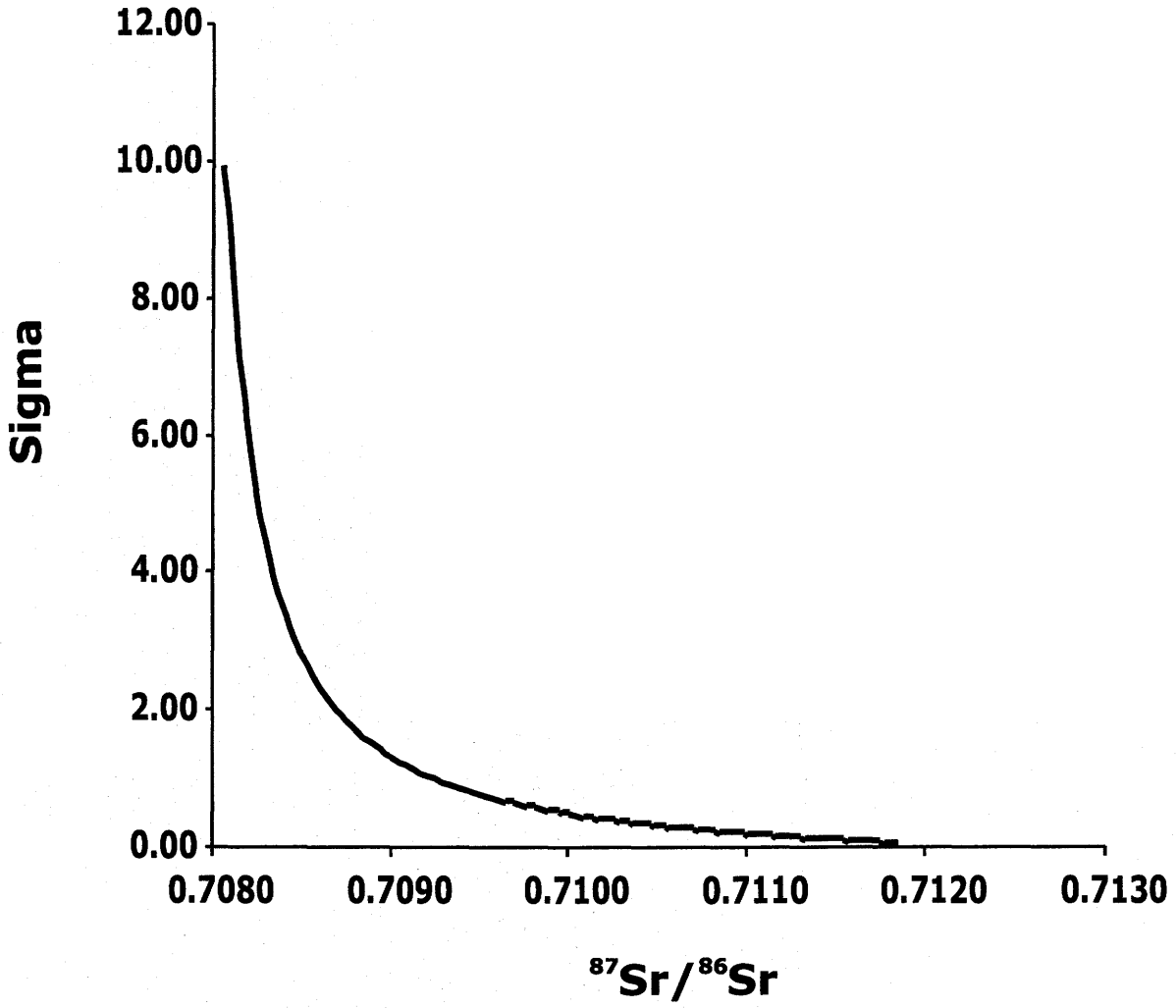

Figure 2-8. Error curve for Figure 2-7, showing $^{87}Sr/^{86}Sr$ vs. Sigma based on 20th and 80th percentile data.

greater impact on the accuracy of paleosalinities from the Sr concentration of freshwater than there is from the Sr concentration of seawater.

2.3.4 Coupled $^{87}Sr/^{86}Sr$ – Ca/Sr

Because the $^{87}Sr/^{86}Sr$ method of paleosalinity determination is based on the assumption of two-component mixing, the coupled $^{87}Sr/^{86}Sr$ – Ca/Sr technique will be used to directly test the premise that salinity in the studied area is controlled by seawater – freshwater mixing.

Seawater and freshwater have very different Sr/Ca ratios; seawater has a 1000Sr/Ca ratio of 8.5 (DeVilliers *et al.*, 1993), while the freshwater 1000Sr/Ca ratio typically ranges between 0.5 and 5.0 (Odum, 1957), with a median value of 2.3 (Holmden *et al.*, 1997). The species-specific Sr distribution coefficient, $D_{Sr} = Sr/Ca_{Shell} / Sr/Ca_{Water}$, allows quantification of the kinetically controlled incorporation of Sr into the mollusk shell (Kulp *et al.*, 1952; Holmden *et al.*, 1997). In addition to the D_{Sr}, the uptake of Sr into the mollusk shell is controlled by the Sr/Ca ratio of the depositional waters (Kulp *et al.*, 1952), the mollusk's growth rate (Purton *et al.*, 1999), and water temperature (e.g. Lowenstam, 1961; Smith *et al.*, 1979). As long as potential variations from growth rate and temperature are smaller than the Sr/Ca variations in the original depositional waters, the value of Sr/Ca_{water} can be extrapolated from a single fossil species using biologically reasonable assigned D_{Sr} values. Modern freshwater aragonitic D_{Sr} values are known to vary from 0.22 to 0.29 (Odum, 1951; Faure *et al.*, 1967; Buchardt & Fritz; 1978), and to range as high as 0.33 (Rosenthal & Katz, 1989; Graham *et al.*, 1982), while marine aragonitic D_{Sr} values may be as low as 0.15 ± 0.02 (Rosenthal & Katz, 1989). Using the coupled $^{87}Sr/^{86}Sr$ – Ca/Sr method, D_{Sr} values for a single species can be determined from several individuals spanning part of the salinity range. On a plot of $^{87}Sr/^{86}Sr$ vs. Ca/Sr,

these fossils would define a linear mixing line, and the fact that seawater must fall on this mixing line can be used to determine the species-specific D_{Sr}. The problem with applying this strategy to ancient environments is that the Sr/Ca ratio of ancient seawater is difficult to determine. This uncertainty translates directly to the uncertainty estimate for D_{Sr}.

3.0 EXPERIMENTAL DESIGN

Fossil bivalve and brachiopod material was collected by Dr. Paul Johnston (Royal Tyrrell Museum, Drumheller, Alberta) on Melville Island, in the Canadian Arctic. Samples were selected from two geographic locations on the island; *Montanaria* sp. was collected from the Hecla Bay Formation at Ibbett Bay, and all other specimens were collected from the underlying Weatherall Formation at McCormick Inlet (figures 2-1 and 2-6). With the exception of *Montanaria* sp., individual shells from single handsamples taken from individual storm lag deposits were selected for analysis. Handsamples were chosen from siliciclastic lithologies and contain little to no carbonate cement. In the case of *Montanaria* sp., individual shells were collected from a single shell bed but not from a single handsample. Matrix and detrital material were removed from the specimens by scraping with dental tools under a microscope, and only clean inner shell fragments were selected for geochemical analysis.

Preservation of shell microstructure was evaluated using a JEOL JSM-840A scanning electron microscope (SEM). 300 μm thick sections were prepared for cathodoluminescence in order to evaluate diagenetic influence. Major element analysis was performed on a Perkin-Elmer ELAN 5000 ICP-MS. Mineralogical evaluation was performed on a Rigaku Rotaflex RU-200 using traditional powder mount techniques. For X-ray diffraction (XRD) analysis, mixtures of aragonite and calcite powder were prepared by weight and analysed, then used to create a calibration curve of peak intensity ratio vs. aragonite content (Figure 3-1), according to the method of Davies &

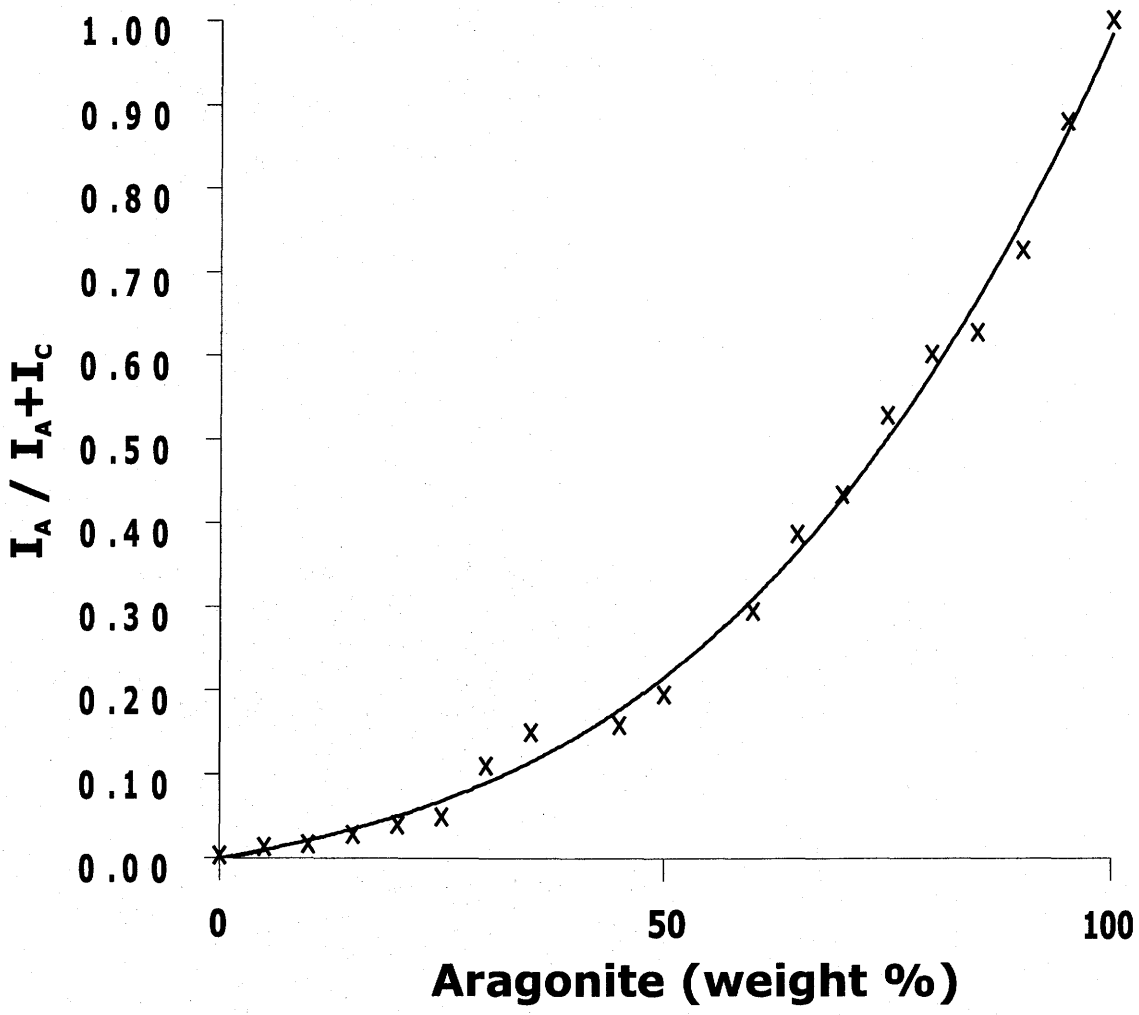

Figure 3-1. Powder mount XRD aragonite calibration curve. "$\mathbf{I_A}$" refers to intensity of the double aragonite peaks (located at 25.5° and 26.5°) and "$\mathbf{I_c}$" refers to the intensity of the calcite peak located at 29.5°.

Hooper (1963). The aragonite and calcite powders were sieved and mixed well to assure homogeneity of the mixture. Peak intensity results for the fossils were then applied to this curve in order to graphically determine the amount of aragonite remaining in the shell specimens. In addition, a new technique, the digitisation of XRD films (O'Neill *et al.*, 1993; Palmer, 1997; Barwood, 2000), involving the little-used Gandolfi method, was employed to qualitatively assess the dispersal of preserved aragonite in the specimens. The Gandolfi technique involves mounting individual sample grains, approximately 1 mm^2 in size, on filaments within a Gandolfi camera. The resulting film strips were then digitised using Image-J (NIH, 2000) to produce a pixel intensity profile (Figure 3-2). In preparation for stable isotope analysis, samples were digested in 100% phosphoric acid, modified after the method of McCrea (1950), using a micro-digestion inlet system, which allows for analysis of samples down to 50 μg in size. The resultant carbon dioxide was analysed on a Finnigan MAT 251 gas isotope ratio mass spectrometer. Unless otherwise stated, oxygen isotope values are reported relative to Pee Dee Belemnite (PDB), as is carbon isotope data. Standard δ notation is used for both, where

$$\delta = (R_{sample}/R_{standard} - 1) \times 1000 \quad (3.1)$$

and

$$R = {}^{13}C/{}^{12}C \text{ or } {}^{18}O/{}^{16}O \quad (3.2)$$

Repeated analyses of NBS-19 during the course of this study yielded 1.94 ± 0.19 (σ) $^{o}/_{oo}$ (n=30) for $\delta^{13}C$ and –2.35 ± 0.17 (σ) $^{o}/_{oo}$ (n=30) for $\delta^{18}O$.

For time series analysis, shell powder aliquots of approximately 50 μg were milled out of shell thin sections, parallel to growth lines, using an electronic micromilling apparatus (EMMA). Oxygen and carbon isotope analyses were performed on the collected

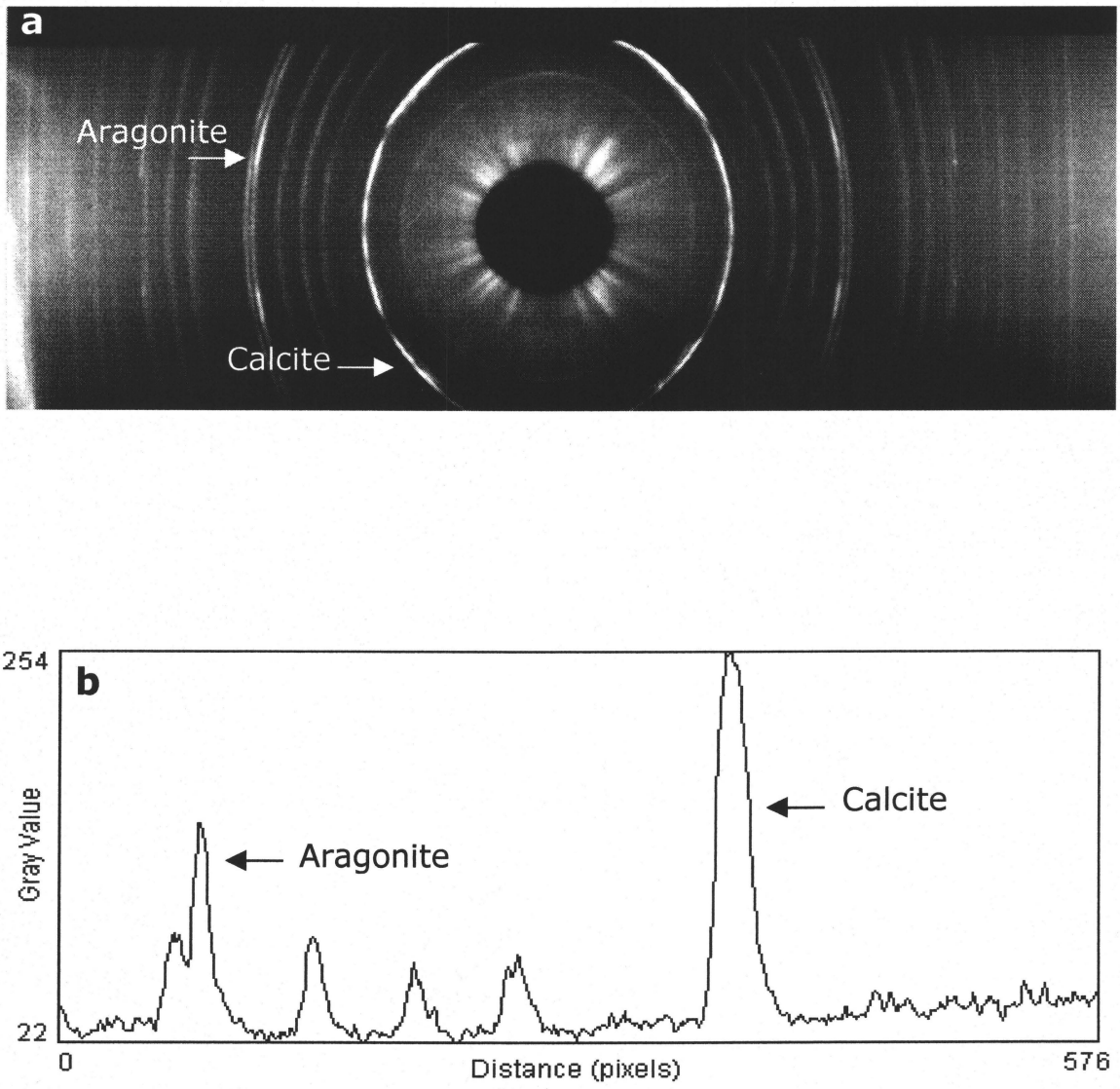

Figure 3-2. (a) X-ray diffraction pattern from a single grain of *Montanaria* sp. (TMP 87.171.02) mounted on a rotating filament and recorded on cylindrical film. (b) Intensity profile generated from (a), showing distinct aragonite and calcite peak patterns.

powders using the microdigestion inlet system of the Finnigan MAT 251, as described above.

In preparation for strontium and calcium isotope dilution and strontium isotope ratio analysis, clean individual shell fragments were dissolved in 1.5N hydrochloric acid. Weighed aliquots of the resulting solutions were then spiked with a weighed amount of ^{48}Ca-^{42}Ca-^{84}Sr tracer solution, dried down and converted to nitrate salts for analysis of Sr/Ca ratio and Ca and Sr concentration by isotope dilution mass spectrometry, using a double filament technique. For strontium isotope ratio determination, aliquots of the same samples were passed through a cation column to separate strontium from calcium and then loaded onto single tantalum filaments with Ta-Gel and analysed on a Finnigan MAT 261 TIMS.

Ca isotope measurements were performed by single collector peak hopping in a cycle consisting of $^{40}Ca - ^{42}Ca - ^{44}Ca - ^{48}Ca$. Care was taken to ensure that peak tailing from ^{39}K onto ^{40}Ca was negligible, even though the abundance measurement of ^{40}Ca does not factor into the isotope dilution calculation. Nevertheless, monitoring the $^{40}Ca/^{44}Ca$ ratio provided an internal check on the performance of the mass spectrometer and accuracy of the fractionation correction.

Sr isotope measurements for isotope dilution analysis were performed on the same filament-load by increasing the temperature of the ionisation filament. Measurements were performed via static multicollection of $^{84}Sr - ^{86}Sr - ^{87}Sr - ^{88}Sr$ and correction of measured ion beam intensities for differences in amplifier gain. Strontium isotope measurements were normalised for variable mass-dependant isotope fractionation to a $^{86}Sr/^{88}Sr$ ratio of 0.1194. Unless otherwise stated, Sr/Ca ratio refers to one thousand times the Sr/Ca atom ratio (mmol/mol).

4.0 RESULTS AND DISCUSSION

4.1 Diagenesis

Evidence that measured chemical and isotopic compositions have not been substantially overprinted by diagenesis is necessary to accurately interpret environmental, chemical and isotopic signatures from the carbonate fossils of the Weatherall and Hecla Bay formations. Because of differences in trace element distribution coefficients between aragonite and calcite, as well as the possibility of pore fluid equilibrium with diagenetic mineral phases, when contemplating the potential for preservation of original environmental signatures, the conversion of these initially aragonitic specimens to calcite must be considered. Under conditions of very low water/rock ratios, however, the trace element concentrations and Sr, O and C isotope compositions may have been, for the most part, conserved during transformation of aragonite to calcite. To assess the extent of variance from their original composition due to diagenesis, the fossils were subjected to (1) scanning electron microscope (SEM) study of microstructure preservation, (2) X-ray diffraction analysis of primary aragonite retention, (3) O isotope time series analysis, (4) trace element abundance analysis, (5) cathodoluminescence, and (6) bulk stable isotope analysis.

4.1.1 Scanning electron microscopy

The bivalve mollusk shell consists of a pair of layered calcium carbonate valves composed of crystalline calcite and/or aragonite (e.g. Bøggild, 1930; Carter, 1990a; Clarkson, 1994). While some bivalve shells are composed entirely of aragonite, the

majority of modern specimens are made up of layers of both calcite and aragonite (e.g. Bøggild, 1930; Clarkson, 1994). The shell's microstructure consists of the patterned arrangement of crystalline calcium carbonate microstructural components, such as tablets and blades, within the shell layers (e.g. Carter, 1990a), and is seldom completely preserved in very ancient fossils (e.g. Clarkson, 1994) due to the diagenetic processes of dissolution and recrystallization.

Scanning electron microscopy was used to study the microstructure of the carbonate fossils of the Weatherall and Hecla Bay formations. *Limoptera* sp. displayed nacreous inner shell layers, consistent with the findings of Taylor *et al.* (1969) and Carter (1990b). *Montanaria* sp. showed crossed lamellar shell layers, similar to those of modern aragonite bivalves (Figure 4-1).

Under high water/rock ratio (open-system diagenesis) conditions, widespread sparry calcite from recrystallization of shell material would be expected. While examples of calcite recrystallization and spar are evident in places, the great majority of shell microstructure remains intact. Such fine preservation of shell microstructure suggests that transformation of aragonite to calcite occurred under conditions of relatively low water/rock ratios (solid-state aragonite neomorphism), such that the secondary calcite was formed predominantly of ion constituents cannibalised from the aragonite (Maliva & Dickson, 1992).

4.1.2 X-ray diffraction

As most of the studied specimens were presumed to be originally aragonitic, XRD analysis was performed to determine whether any aragonite has been preserved. Results of XRD powder diffraction analysis, shown in Table 4-1 and Appendix I,

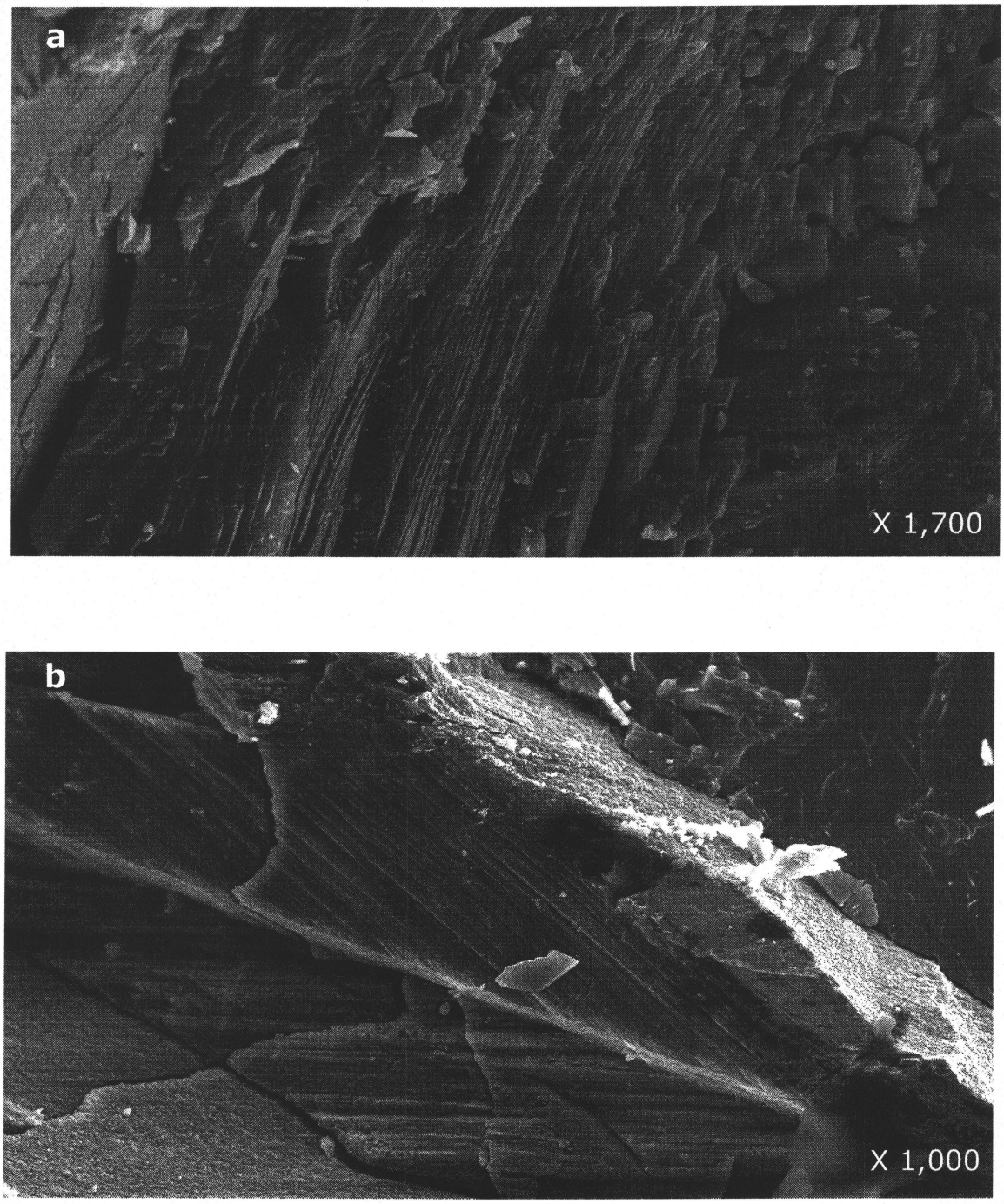

Figure 4-1. (a) SEM photo of radial section of *Limoptera* sp. showing nacre with some tablets diagenetically fused together (J. Carter, personal communication; 2001). (b) SEM photo of vertical section of *Montanaria* sp. showing first order lamellae of crossed lamellar or complex crossed lamellar structure, as well as their second order lamellae (J. Carter, personal communication; 2001).

Table 4-1. Mineralogy results for selected carbonate fossils of the Weatherall and Hecla Bay formations.

Sample name	**% aragonite**
Nuculopsis sp.	
TMP 87.162.2-1	16
Nyassidae n. gen. & n. sp.	
U of A P908-1	12
Montanaria sp.	
TMP 87.171.02-1	18

indicate that the samples contain up to 18% aragonite. Results of Gandolfi X-ray diffractometry, however, suggest that this relic aragonite, thus far the oldest preserved in the rock record, is preserved on the millimetre scale and, thus, physically inextricable from the encasing diagenetically precipitated calcite.

4.1.3 Time series analysis

Time series analyses are used to trace the seasonal variations of O isotope composition throughout the lifetime of one specimen. Modern bivalve time series often exhibit a sinusoidal variation of $\delta^{18}O$, which can be attributed to temperature effects and/or variation in the isotopic composition of the water (Urey *et al.*, 1951; Epstein & Lowenstam, 1953; Keith & Parker, 1965; Grossman & Ku, 1986; Krantz *et al.,* 1987; Arthur *et al.,* 1983; Jones, 1998; Geary *et al.,* 1992). This phenomenon can also be used to assess diagenetic alteration; as a result of diagenesis, the original pattern of seasonal $\delta^{18}O$ variation will be smoothed out or even obliterated altogether, reflecting the homogenisation of the O isotope content throughout the shell.

Oxygen isotope time series from *Limoptera* sp. (Figure 4-2) show part of a pattern of sinusoidal $\delta^{18}O$ variation with an amplitude of 2 $^{o}/_{oo}$. Preservation of this pattern is evidence that *Limoptera* sp. has undergone relatively closed-system (solid-state) diagenesis.

Using the temperature-dependent carbonate-water equilibrium isotope fractionation equation of O'Neill *et al.* (1969), the 2 $^{o}/_{oo}$ $\delta^{18}O$ variation evident from the shell time series translates to a temperature variation of 8° C, if the $\delta^{18}O$ of the habitat waters is assumed to be constant. During the Devonian, Melville Island was a tropical environment, located within approximately 20° of the equator (Ziegler, 1988; Scotese

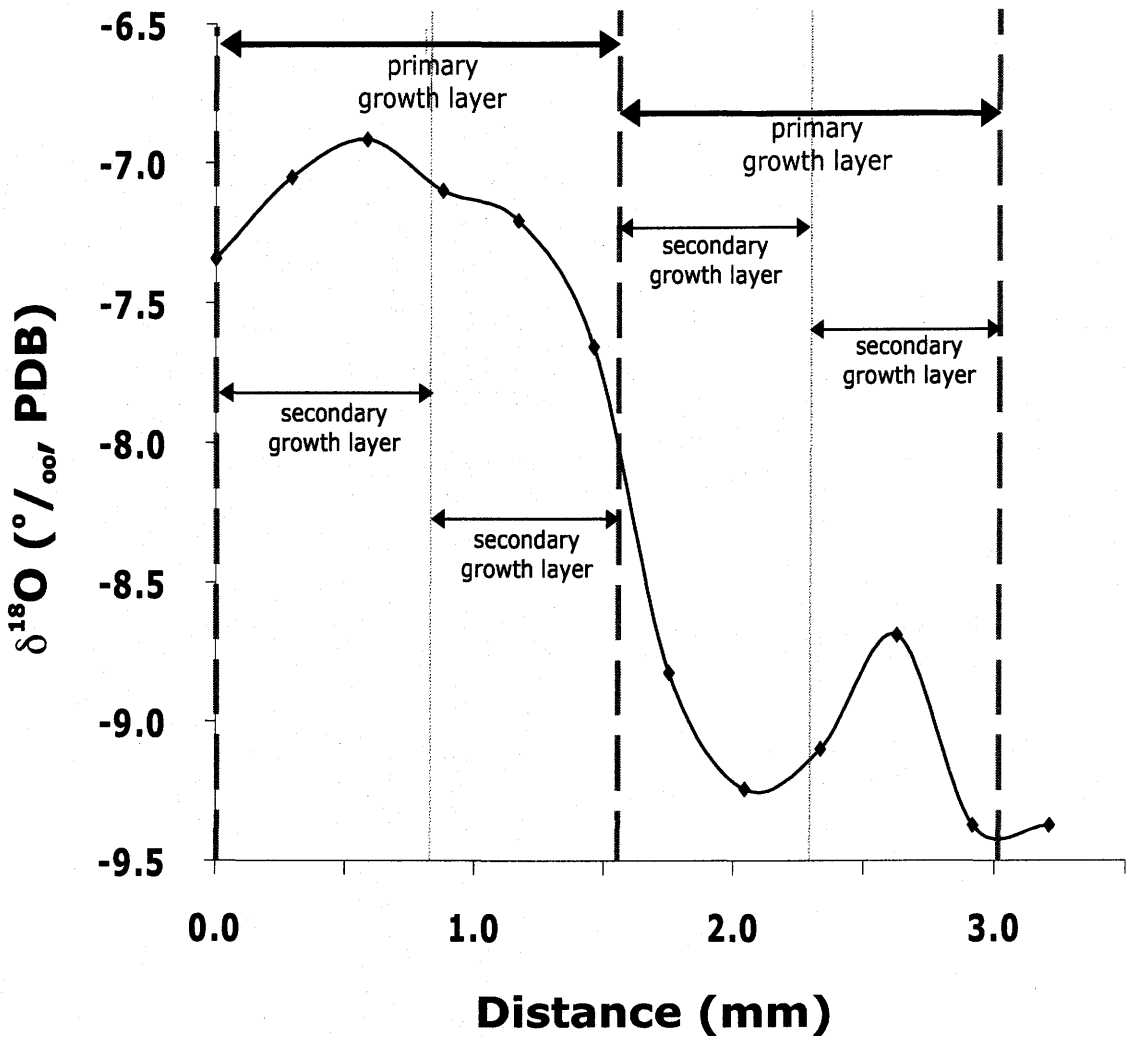

Figure 4-2. Time series analysis of $\delta^{18}O$ (PDB) values from primary and secondary growth layers of *Limoptera* sp. (U of A P904).

and McKerrow, 1990; Scotese, 2000). Because Devonian sea surface temperatures are unknown, early Cenozoic and modern equatorial sea surface temperatures will be used to estimate a paleotemperature range for the depositional waters of Melville Island in the Middle Devonian. In the early middle Eocene, equatorial Atlantic sea surface temperatures ranged from an average of 25° C in the winter months, to 28° C in the summer months (Andreasson and Schmitz, 2000). Similarly, in the modern Atlantic Ocean, average sea surface temperatures range from approximately 24° C in the winter, to 28° C in the summer (Levitus and Boyer, 1994, as reported in Andreasson and Schmitz, 2000; Flament, 1996), within 20° of the equator.

Based on this information, a paleotemperature range of $\Delta T = 4°$ C is reasonable for Melville Island in the Middle Devonian. A portion of the $\delta^{18}O$ signal, therefore, likely reflects salinity variations due to seawater-freshwater mixing (Epstein & Lowenstam, 1953; Dodd & Stanton, 1975; Jones *et al.*, 1978; Arthur *et al.*, 1983; Geary *et al.*, 1992), or degrees of potential evaporative enrichment of ^{18}O in the habitat waters, which may equal, or outweigh, assumed temperature variations at the studied latitude. Thus, the complex interplay between temperature, evaporation and salinity variations in carbonate $\delta^{18}O$ values must be considered while interpreting these isotopic time series.

4.1.4 Trace element analysis

Trace element discrimination diagrams have been used extensively to assess the degree of preservation of marine fossils' chemical and isotopic compositions (e.g. Veizer, 1977; Brand & Veizer, 1980; Brand, 1981; 1983; Brand & Morrison, 1987; Brand *et al.*, 1993; Brand, 1994). Such evaluations are based on comparison of the trace element composition of ancient marine fossils with modern marine equivalents, where fossils

with compositions that plot outside the modern marine domains are considered altered. Furthermore, covariant trends on such plots are widely considered to be evidence for diagenetic disturbance, as they are believed to reflect mixtures of pristine and altered materials in the fossils. The two most important diagenetic indicators are Fe and Mn. This approach is difficult to apply to brackish or non-marine fauna because shell precipitation in non-marine environments may result in more or less incorporation of certain trace elements into shell carbonate than in the marine environment (Brand & Morrison, 1987), due to the differences in elemental concentration between fresh and marine waters. Thus, what are, in fact, environmental trends in brackish water chemistry preserved in shells of brackish dwelling fauna may be mistaken for diagenetic trends. Even Fe and Mn, which are very diagnostic of alteration, are unreliable in brackish fauna because freshwater can contain significantly higher Fe and Mn concentrations than seawater. The concentration of Fe and Mn in brackish waters can be further elevated by salinity stratification and development of suboxic bottom waters where redox sensitive Fe and Mn are more soluble. The suboxic interstitial waters of Saanich Inlet, British Columbia, for example, have Fe and Mn concentrations substantially higher than open ocean water; while seawater contains, on average, 6×10^{-5} ppm Fe and 3×10^{-4} ppm Mn (Faure, 1991), the interstitial waters of Saanich Inlet (0 to 15 cm from the sediment-water interface) contain up to 1.20×10^{-4} ppm Fe and 1.00×10^{-3} ppm Mn (Presley *et al.*, 1972). As the Melville Island fossils are thought to have been precipitated within the seawater – freshwater mixing zone, covariant trends in trace elements and isotopes recorded in the shells may actually reflect the original range of elemental and isotopic abundances in the brackish depositional water. It is therefore important to recognize that

differentiation between diagenetic trends and original environmental trends is not straightforward when dealing with brackish water fauna.

This is further complicated by the fact that the fossils have mostly been recrystallized as calcite, likely resulting in some trace element exchange with diagenetic fluids. Due to the high Sr content of aragonite relative to calcite, under diagenetic conditions, the dissolution of aragonite and precipitation of diagenetic calcite normally results in decreased Sr and Na concentrations and uptake of Fe, Mn and Mg from the diagenetic fluid (e.g. Brand & Morrison, 1987).

There is very little trace element data available for ancient non-marine aragonite bivalves. The primarily deltaic and shallow marine Upper Carboniferous members of the Breathitt Formation in southeastern Kentucky, however, contain aragonite bivalves which have undergone little alteration (e.g. Dennis & Lawrence, 1979; Brand, 1981; 1983; Brand & Morrison, 1987; Carter, 1990b). These mollusks have been widely studied and can therefore be used as analogues.

Results of trace element analysis of selected carbonate fossils of the Weatherall and Hecla Bay formations are listed in Table 4-2. The fossils display relatively high Sr and Na concentrations, similar to modern values for aragonite mollusks from marine (Brand *et al.*, 1987) and freshwater environments (Rosenthal & Katz, 1989), while Fe, Mn and Mg concentrations are higher than modern marine values (Table 4-2). The preservation of high Sr concentrations, in particular, indicates that diagenesis occurred under relatively closed-system conditions, and suggests that other elemental signatures may be partially preserved, while the fossils' high Fe and Mn contents may, in part, indicate growth in waters low in dissolved oxygen (e.g. Veizer, 1977; Brand, 1987; Brand, 1989; Brand, 1994).

Table 4-2. Trace element data for selected carbonate fossils of the Weatherall and Hecla Bay formations.

Sample name	Fe ppm	Mn ppm	Sr ppm	Na ppm	Mg ppm	Ba ppm
I. Weatherall Formation						
McCormick Inlet						
Montanariidae n. gen. & n. sp.						
TMP 87.162.3-1	9591.9	3290.3	722.4	2284.0	1706.5	108.6
TMP 87.162.3-2	11809.9	4192.6	949.5	2116.6	1921.0	154.9
TMP 87.162.3-3	7358.6	2487.8	1413.6	2362.7	1715.7	198.5
TMP 87.162.3-4	12262.9	3974.8	1051.7	2576.7	2447.2	150.1
Nyassidae n. gen. & n. sp.						
U of A, P906 Cyc. 1	8222.3	3927.6	1576.5	2263.2	1854.6	203.6
U of A, P906 Cyc. 2	10225.0	4714.0	1529.6	2858.9	1990.4	240.8
U of A, P906 Cyc. 3	9306.3	4230.5	1504.4	2749.8	2028.5	229.7
U of A, P906 Cyc. 4	6958.0	3031.4	1348.5	1651.7	2079.5	201.4
Limoptera sp.						
U of A, P906 Lim. 1	540.1	390.5	1293.8	2061.2	379.2	36.0
U of A, P906 Lim. 2	4633.7	3205.1	941.8	2197.4	811.2	92.6
U of A, P906 Lim. 3	617.0	862.9	1418.9	2330.2	375.6	67.9
U of A, P906 Lim. 4	117.1	411.9	1396.2	2166.8	410.9	57.4
U of A, P906 Lim. 5	9681.1	6658.5	991.7	3251.7	1537.2	141.6
U of A, P906 Lim. 6	3430.8	3077.0	1199.0	3399.4	756.0	74.8
U of A, P906 Lim. 7	14632.4	12582.3	583.9	1776.9	1488.3	112.3
U of A, P906 Lim. 8	6132.2	4767.9	1129.9	2819.0	996.5	125.3
Ibbett Bay						
Atrypa sp.						
TMP 1987.174.2	761.1	1042.1	462.3	3898.4	564.7	13.4
II. Hecla Bay Formation						
Ibbett Bay						
Montanaria sp.						
GSC C-140085-1	7136.9	1712.7	909.6	527.1	1515.1	34.9
GSC C-140085-2	11478.6	2203.7	1003.7	434.0	2214.0	9.6
GSC C-140085-3	4836.2	1233.3	879.2	915.4	865.9	17.5
GSC C-140085-4	4365.5	844.8	1346.9	313.3	1503.0	12.3
Diagenetic calcite						
milled from TMP 87.171.02-3	7989.5	302.3	418.2	4109.9	2552.2	189.9
III. Modern aragonite bivalves						
data from Brand *et al* ., 1987	20-130	3-14	840-2890	2200-6320	50-890	

* highlighted samples were used for the $\delta^{18}O$ mixing line.

In a plot of Fe vs. Mn (Figure 4-3), the Melville Island bivalves plot in the fluvial, suboxic zone (Brand, 1994). As only clean sample pieces from the inner shell layers were selected for geochemical analysis, the specimens' high Fe content cannot be attributed to Fe coatings on the fossils.

Although the largely recrystallized bivalves of the Weatherall and Hecla Bay formations contain concentrations of Fe and Mn much higher than modern marine specimens, their trace element geochemistry is quite similar to that of the relatively well-preserved aragonite mollusks of the Breathitt Formation (figures 4-4 & 4-5). These results suggest that the depositional waters for both the Breathitt Formation and the Weatherall and Hecla Bay formations contained substantially higher levels of dissolved Fe, Mn and Mg than seawater, as is the case for the suboxic waters of Saanich Inlet, British Columbia (Presley *et al.*, 1972). This points to a potential environmental cause of elemental enrichment in addition to that which may be attributable to diagenesis, making it difficult to assess the degree of diagenetic impact on the Melville Island specimens from trace element analyses. The Melville Island mollusks contain slightly higher amounts of Mg than the Breathitt Formation bivalves (Figure 4-6). This is probably due to the more recrystallized nature of the Weatherall and Hecla Bay samples, as calcite contains more Mg than aragonite.

4.1.5 Cathodoluminescence

Cathodoluminescence is widely used to differentiate diagenetically altered material from pristine material, based on a specimen's trace element geochemistry, in particular its Fe and Mn content.

Cathodoluminescence occurs when, as a result of electron excitation, a photon is emitted

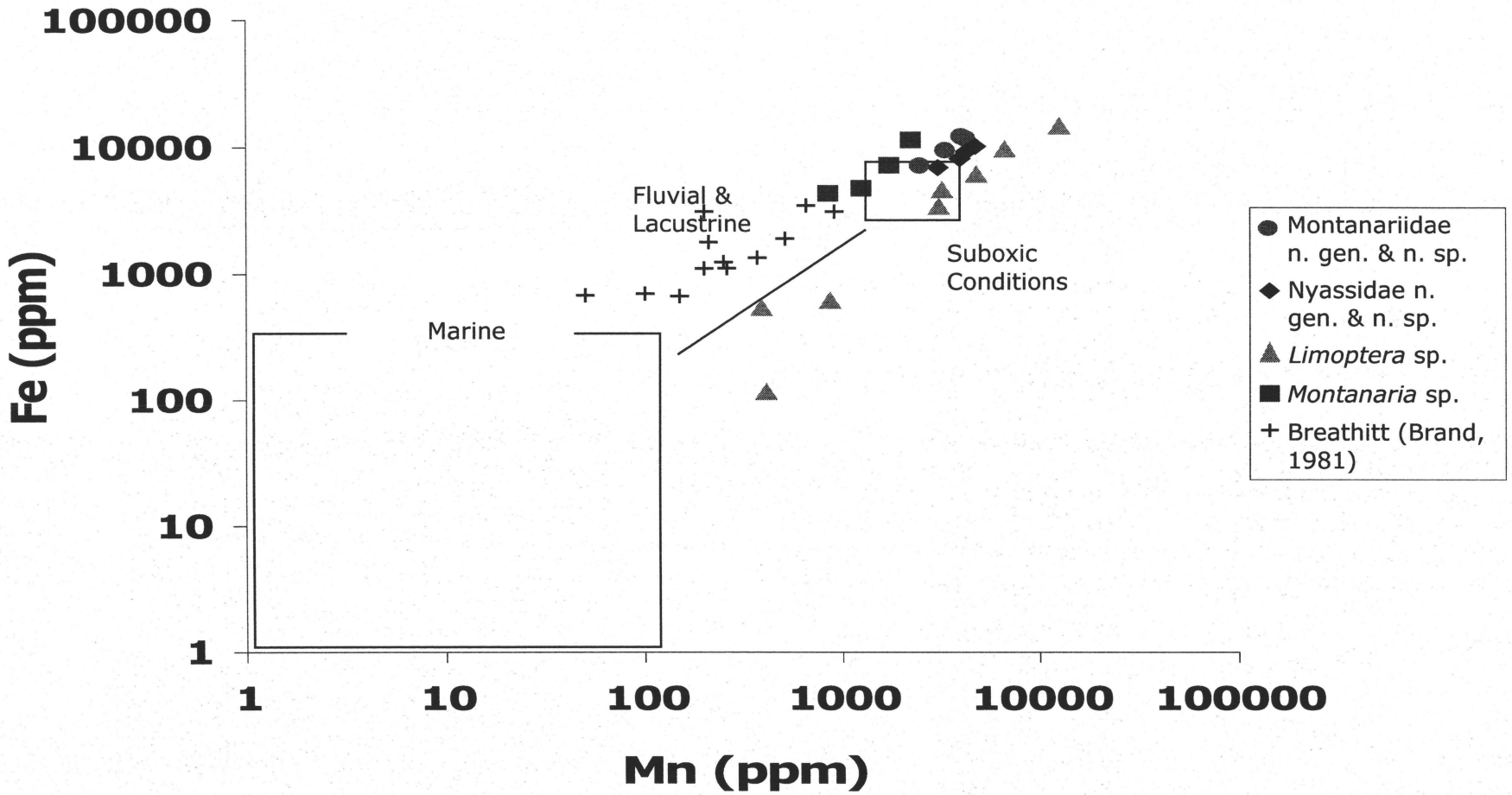

Figure 4-3. Fe vs. Mn for the carbonate fossils of the Weatherall and Hecla Bay formations. Marine aragonite, suboxic, and fluvial & lacustrine zones are based on Brand (1994). Data for the analogous Breathitt Formation mollusks are shown for comparison.

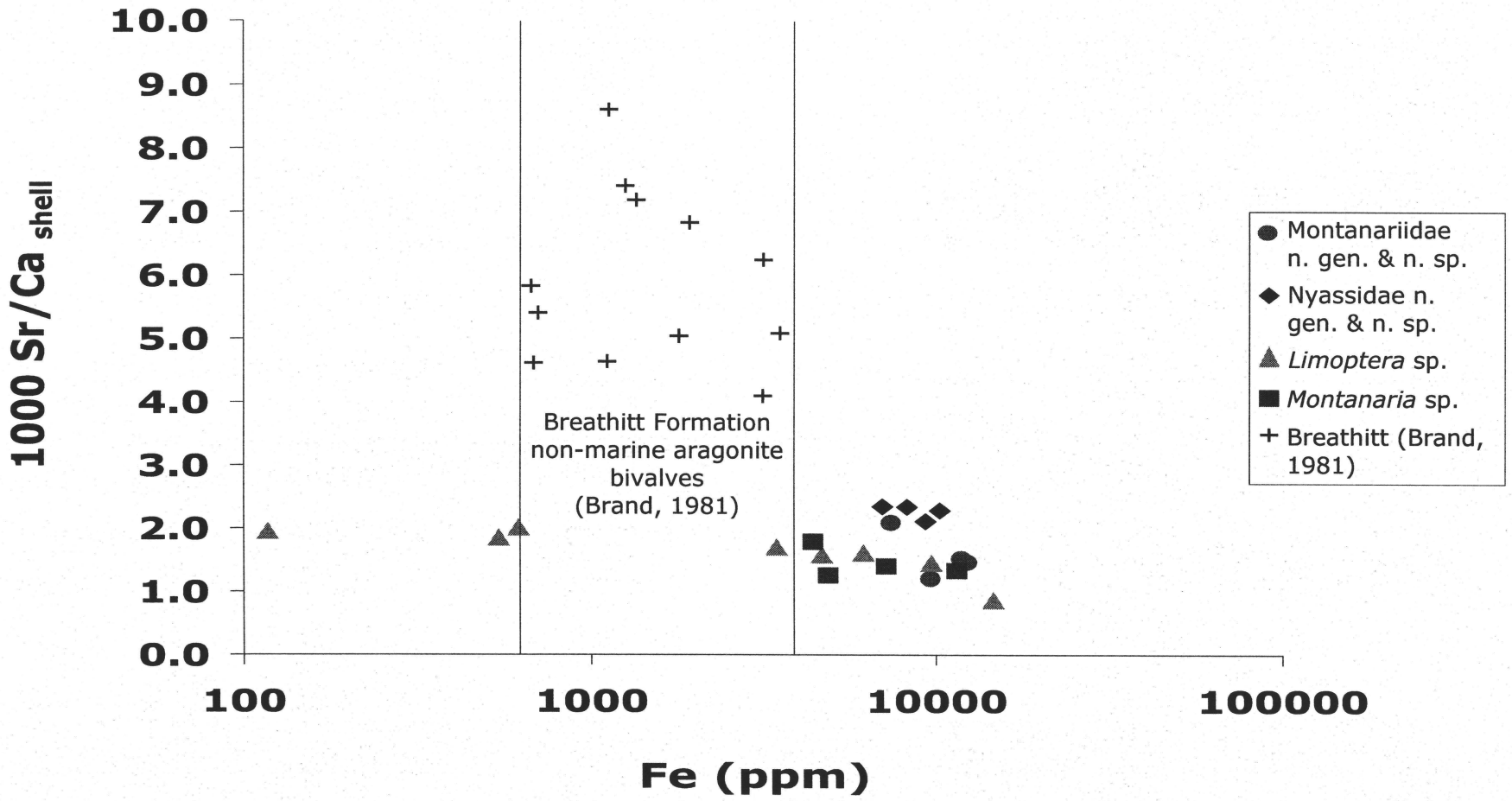

Figure 4-4. Sr/Ca $_{shell}$ and Fe concentration data for carbonate fossils of the Weatherall and Hecla Bay formations. Data for the analogous Breathitt Formation mollusks are shown for comparison.

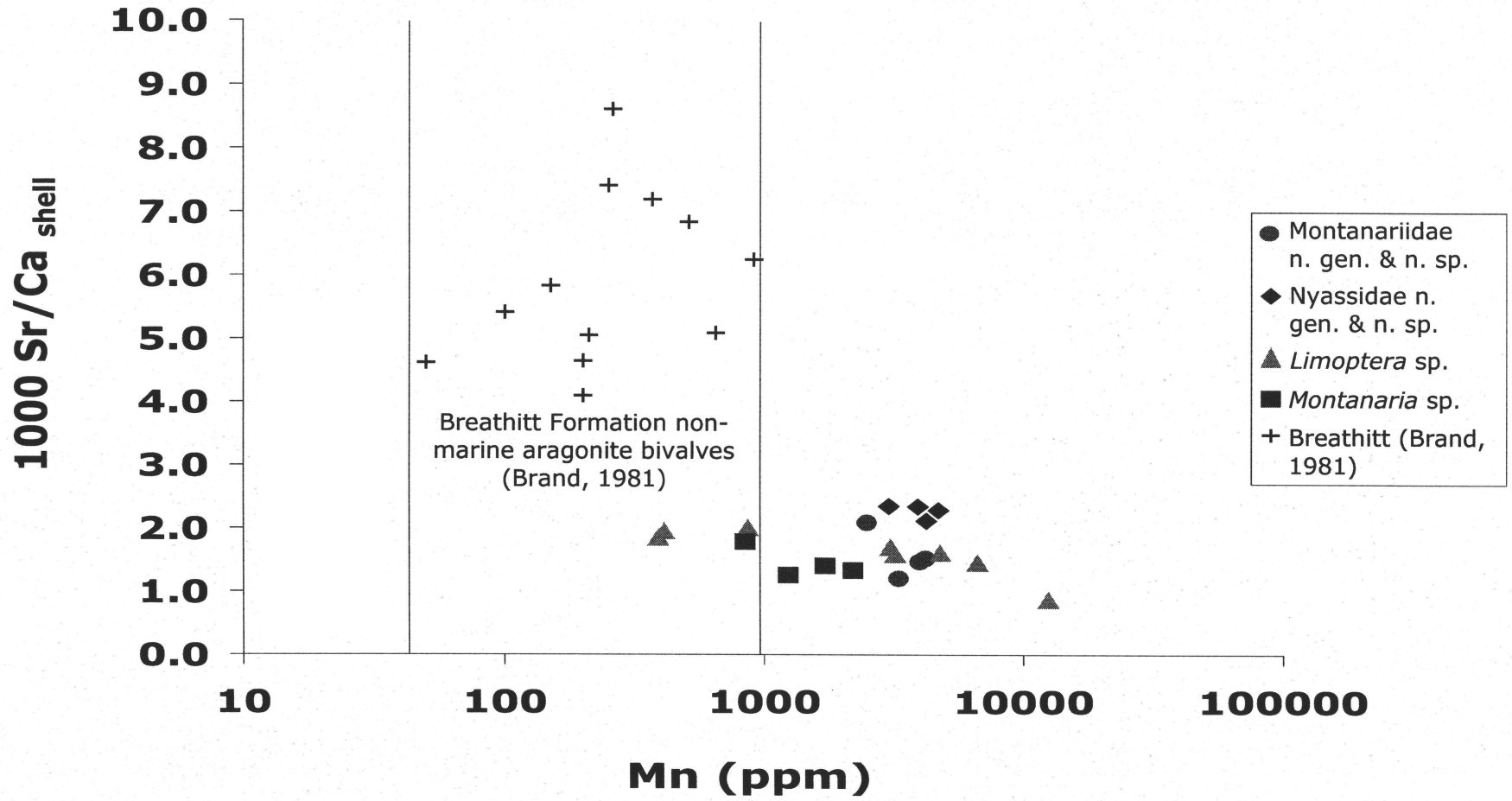

Figure 4-5. Sr/Ca $_{shell}$ and Mn concentration data for carbonate fossils of the Weatherall and Hecla Bay formations. Data for the analogous Breathitt Formation mollusks are shown for comparison.

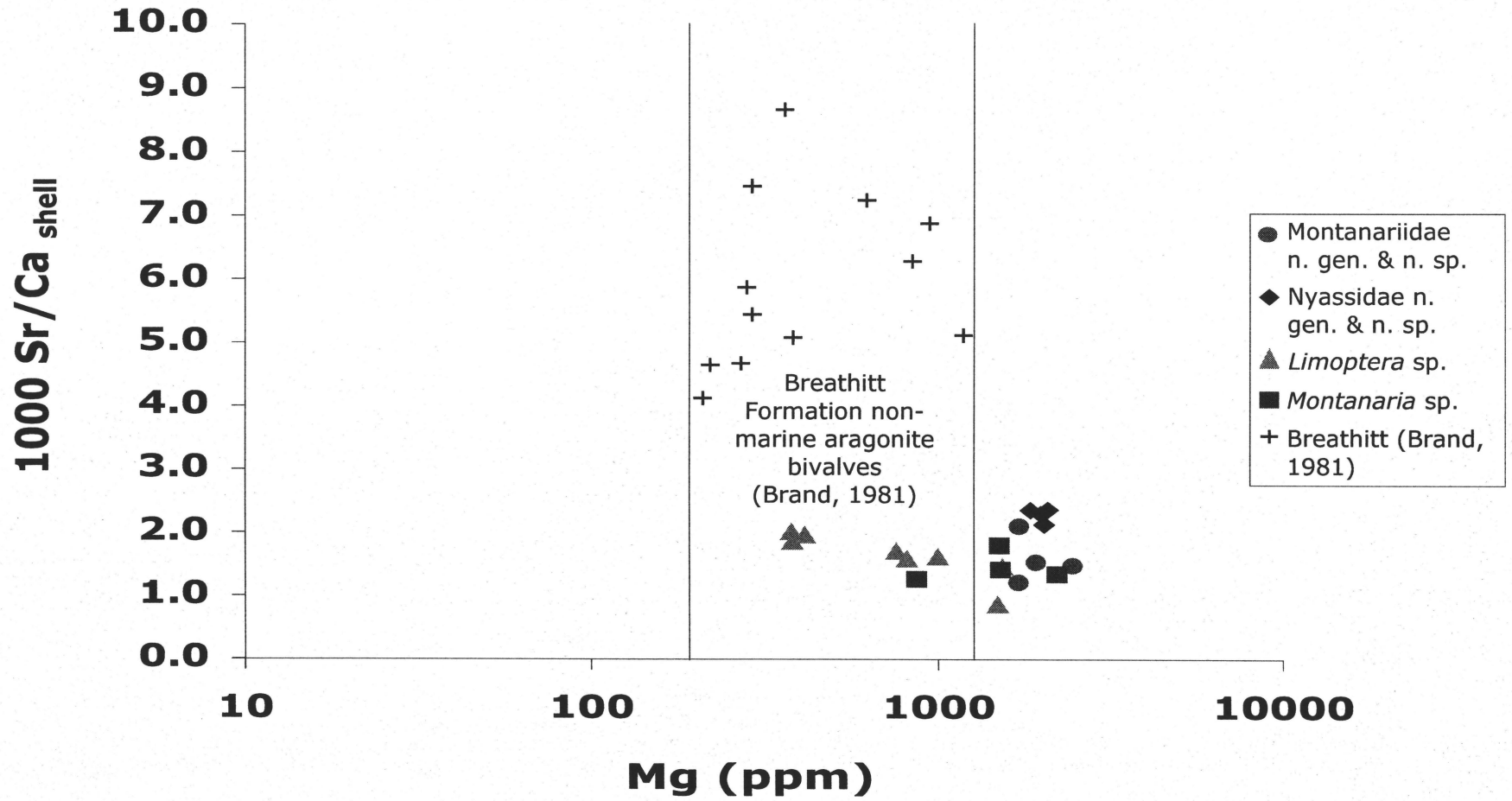

Figure 4-6. Sr/Ca $_{shell}$ and Mg concentration data for carbonate fossils of the Weatherall and Hecla Bay formations. Data for the analogous Breathitt Formation mollusks are shown for comparison.

in the visible range of the electromagnetic spectrum (e.g. Barbin, 2000; Pagel *et al.*, 2000). Activators, trace elements occupying particular sites in the crystal lattice, trigger luminescence in a specimen when a valence electron is captured by the conduction band and, upon its return to the valence band, produces a photon (Pagel *et al.*, 2000). According to the literature, Mn^{2+} is the most important activator in carbonates (e.g. Machel, 1985; Mason, 1987; Habermann *et al.* 2000; Machel, 2000). Quenching, the damping of cathode-ray-induced luminescence is of great importance in the study of diagenetic material. Fe^{2+} is widely believed to be the most important quenching element in carbonates (e.g. Machel, 1985; Mason, 1987; Habermann *et al.* 2000; Machel, 2000). Mn^{2+} activated luminescence can be quenched at 3000 to 4000 ppm Fe (Habermann *et al.*, 2000). The extent of Fe quenching is constrained by the specimen's Mn and Fe concentrations, and the efficiency of Fe quenching increases with Mn content, due to the subsequent decrease in distance between the Fe^{2+} and Mn^{2+} ions (Habermann *et al.*, 2000). Of additional importance is the occurrence of self-quenching, which may result from a specimen's high activator concentration (e.g. Habermann *et al.*, 2000). According to Mason (1997), this phenomenon takes place at >500 ppm Mn, while more recent studies (Habermann *et al.*, 2000) put it at >1000 ppm Mn.

Excepting rare visible occurrences of calcitic spar within the shell material, the shells did not luminesce. While the aforementioned quenching phenomena may be responsible for the lack of luminescence in the majority of samples, some specimens of *Limoptera* sp. (P906-1, P906-3 and P906-4), *Montanaria* sp. (GSC C-140085) and *Atrypa* sp. (TMP 1987-174.2) show Fe and Mn concentrations below the quenching range (Table 4-2).

4.1.6 $\delta^{18}O$, $\delta^{13}C$ and Sr/Ca

The ^{13}C, ^{18}O and Sr content of fossil carbonates may show variation as a result of interaction with diagenetic fluids. Because meteoric waters are depleted of ^{13}C, ^{16}O and Sr relative to seawater, neomorphic calcite which precipitates in an open meteoric setting (high water/rock ratio) will reflect this depletion (Martin *et al.*, 1986; Maliva & Dickson, 1992; Hendry *et al.*, 1995; Maliva, 1998) and may, therefore, reflect the composition of diagenetic fluids rather than the original depositional waters. Typically, alteration leads to decreased ^{13}C, ^{18}O and Sr content, as diagenetic fluids are commonly meteoric. Under such open-system diagenetic conditions, the $^{87}Sr/^{86}Sr$ ratio is driven toward more radiogenic values (higher content of radioactive isotope) and the Sr/Ca content of the skeletal carbonate decreases as aragonite is reprecipitated as diagenetic calcite, which has a lower D_{Sr}.

Shell $\delta^{18}O$ values (Table 4-3) for the carbonate fossils of the Weatherall and Hecla Bay formations are plotted against $\delta^{13}C$ in Figure 4-7. If these were marine fauna, diagenetic trends would commonly be manifested by positive correlation of $\delta^{18}O$ and $\delta^{13}C$, because diagenetic fluids often have a strong meteoric water component characterised by low $\delta^{18}O$ and dissolved inorganic carbon with low $\delta^{13}C$. Once again, when dealing with brackish or marginal marine settings, it is difficult to distinguish original environmental trends in the shells caused by salinity fluctuations from trends caused by diagenetic alteration.

In Figure 4-7, shells displaying relatively good preservation, based on trace element geochemistry, are contained within a circular zone. The arrow indicates the range of

Table 4-3. Oxygen and carbon isotope data for carbonate fossils of the Weatherall and Hecla Bay formations.

Sample name	$\delta^{18}O$ (‰, PDB) (shell)	$\delta^{18}O$ (‰, SMOW) (water)	$\delta^{13}C$ (‰, PDB) (shell)
I. Weatherall Formation			
McCormick Inlet			
Nuculopsis sp.			
TMP 87.162.1-1	-9.5	-6.8	-1.4
TMP 87.162.1-2	-9.0	-6.3	-1.0
TMP 87.162.1-3	-9.7	-7.0	-1.6
TMP 87.162.1-4	-9.7	-7.0	-1.5
TMP 87.162.1-5	-9.7	-7.0	-1.5
TMP 87.162.1-6	-9.4	-6.7	-1.7
TMP 87.162.1-7	-9.8	-7.1	-1.0
Montanariidae n. gen. & n. sp.			
TMP 87.162.3-1	-8.4	-5.7	1.0
TMP 87.162.3-2	-8.5	-5.7	0.2
TMP 87.162.3-3	-8.6	-5.9	0.5
TMP 87.162.3-4	-8.3	-5.6	1.0
Nyassidae n. gen. & n. sp.			
U of A, P906 Cyc. 1	-8.8	-6.1	-1.7
U of A, P906 Cyc. 2	-9.7	-6.9	-1.3
U of A, P906 Cyc. 3	-9.5	-6.8	-1.9
U of A, P906 Cyc. 4	-9.3	-6.6	-1.8
Limoptera sp.			
U of A, P906 Lim. 1	-10.2	-7.5	0.4
U of A, P906 Lim. 2	-9.4	-6.7	-0.7
U of A, P906 Lim. 3	-10.5	-7.8	0.4
U of A, P906 Lim. 4	-10.2	-7.5	0.9
U of A, P906 Lim. 5	-9.0	-6.3	-1.4
U of A, P906 Lim. 6	-9.6	-6.8	0.5
U of A, P906 Lim. 7	-8.8	-6.0	-5.0
U of A, P906 Lim. 8	-10.3	-7.6	-1.2
Ibbett Bay			
Atrypa sp.			
TMP 1987.174.2	-5.0	-2.3	1.2
II. Hecla Bay Formation			
Ibbett Bay			
Montanaria sp.			
TMP 87.171.02-1	-10.5	-7.8	-1.4
TMP 87.171.02-2	-13.1	-10.4	-2.6
TMP 87.171.02-3	-12.6	-9.9	-2.9
TMP 87.171.02-4	-11.3	-8.6	0.9
Montanaria sp.			
GSC C-140085-1	-9.9	-7.2	-0.1
GSC C-140085-2	-7.6	-4.9	-1.6
GSC C-140085-3	-11.7	-9.0	-0.4
GSC C-140085-4	-11.1	-8.4	0.4
Diagenetic calcite			
milled fromTMP 87.171.02-3	-11.1	-8.4	-2.3

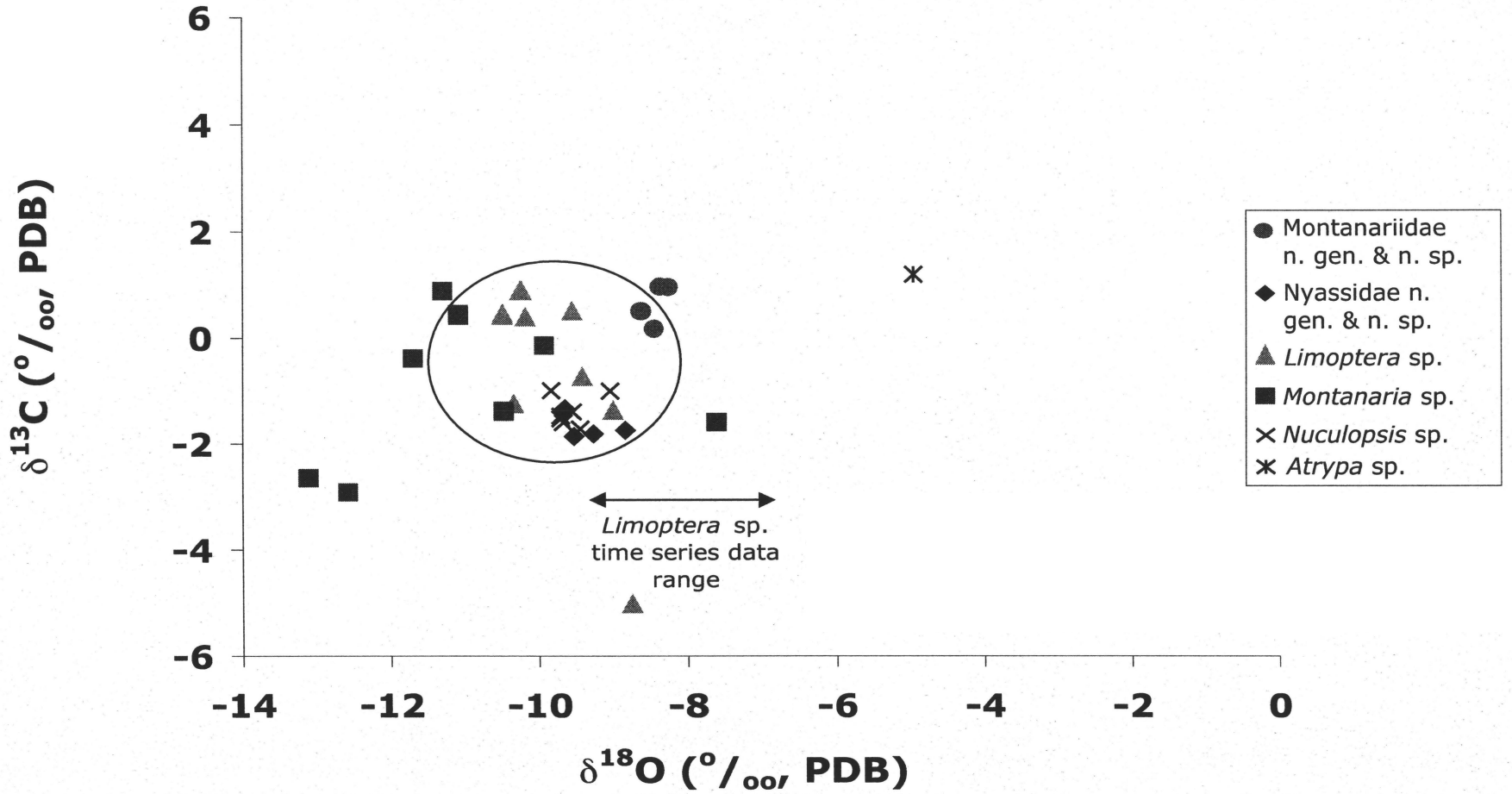

Figure 4-7. Shell $\delta^{18}O$ (PDB) and shell $\delta^{13}C$ (PDB) values for carbonate fossils of the Weatherall and Hecla Bay formations. If environmental trends were present, correlation of the data would be expected, due to the difference in endmembers; seawater would generate high $\delta^{18}O$ and $\delta^{13}C$ values while freshwater would produce low $\delta^{18}O$ and $\delta^{13}C$ values. Likewise, if diagenesis had altered the shells' ^{18}O and ^{13}C content, a correlative trend would be apparent. Relatively well-preserved samples are shown within the circle and the arrow indicates the range of $\delta^{18}O$ variation derived from the time series analysis of *Limoptera* sp.

$\delta^{18}O$ variation derived from time series analysis of *Limoptera* sp. There is an overlap of approximately $1^{o}/_{oo}$ between the two.

In the case of *Limoptera* sp. and, to a lesser extent, that of *Montanaria* sp., there is evident correlation between Sr/Ca (Table 4-4) and $\delta^{13}C$ (Figure 4-8). While this is interpreted as a potential diagenetic trend, it is difficult to rule out that the correlation may be a feature of the brackish seawater-freshwater mixing zone environment.

In summary, the results of SEM, cathodoluminescence, trace element, and isotope geochemistry analyses support the theory of relatively closed-system (low water/rock ratio) diagenesis. However, as quantitative XRD indicates transformation of up to 88% of original shell aragonite to calcite, the difficulty of differentiating environmental trends from diagenetic trends in isotope and trace element patterns in brackish water fauna must be emphasised. It is therefore concluded, conservatively, that the observed trends are diagenetic. These trends will therefore be used for back-extrapolation to isotope and trace element compositions that are more likely to represent genuine environmental signatures.

4.2 Isotope paleohydrology and inferred salinity trends for Melville Island

4.2.1 The $^{87}Sr/^{86}Sr$ – Ca/Sr diagram

The $^{87}Sr/^{86}Sr$ – Ca/Sr diagram can be a very useful plot for extricating potential diagenetic trends from environmental trends. Straight lines on such a plot may be considered the product of two-component mixing. In the case of diagenetic disturbance of the Sr system in shells from a single handsample, individual shells may plot on a straight-line trajectory, which could be interpreted as different degrees of Sr exchange with diagenetic fluids accompanying neomorphism. If neomorphism occurs under low

Table 4-4. Strontium isotope data for carbonate fossils of the Weatherall and Hecla Bay formations.

Sample name	$^{87}Sr/^{86}Sr$ *	Sr ppm	1000 Sr/Ca (shell)	2σ	Ca/Sr (shell)	D_{Sr}	1000 Sr/Ca (water)	Ca/Sr (water)
I. Weatherall Formation								
McCormick Inlet								
Nuculopsis sp.								
TMP 87.162.1-1	0.710367 (07)	1798	2.188	0.0004	457.0	0.33	7.058	141.7
TMP 87.162.1-2	0.710492 (10)	1751	2.156	0.0002	463.9	0.33	6.954	143.8
TMP 87.162.1-3	0.710479 (07)	1926	2.095	0.0001	477.4	0.33	6.757	148.0
TMP 87.162.1-4	0.710283 (07)	2213	2.520	0.0005	396.8	0.33	8.129	123.0
TMP 87.162.1-5	0.709921 (09)	2257	2.697	0.0004	370.7	0.33	8.701	114.9
TMP 87.162.1-6	0.710528 (09)	1927	2.132	0.0005	469.0	0.33	6.879	145.4
TMP 87.162.1-7	0.709847 (11)	2183	2.503	0.0008	399.6	0.33	8.073	123.9
Nuculopsis sp.								
TMP 87.179.1-1	0.711162 (08)	1591	2.087	0.0010	479.1	0.33	6.325	158.1
TMP 87.179.1-2	0.711380 (12)	1630	1.904	0.0000	525.2	0.33	5.770	173.3
TMP 87.179.1-3	0.711789 (09)	1815	2.137	0.0002	468.0	0.33	6.475	154.4
TMP 87.179.1-4	0.710173 (10)	2153	2.606	0.0000	383.8	0.33	7.896	126.6
Montanariidae n. gen. & n. sp.								
TMP 87.162.3-1	0.711200 (12)	912	1.208	0.0002	828.0	0.26	3.896	256.7
TMP 87.162.3-2	0.711679 (26)	1134	1.524	0.0001	656.4	0.26	4.915	203.5
TMP 87.162.3-3	0.710622 (09)	1677	2.093	0.0001	477.7	0.26	6.752	148.1
TMP 87.162.3-4	0.711728 (27)	1196	1.470	0.0045	680.2	0.26	4.743	210.9
Nyassidae n. gen. & n. sp.								
U of A, P906 Cyc. 1	0.710667 (08)	1931	2.342	0.0006	427.0	0.31	7.555	132.4
U of A, P906 Cyc. 2	0.711105 (09)	1753	2.281	0.0004	438.4	0.31	7.358	135.9
U of A, P906 Cyc. 3	0.710969 (10)	1741	2.115	0.0003	472.8	0.31	6.823	146.6
U of A, P906 Cyc. 4	0.710958 (11)	1815	2.346	0.0005	426.3	0.31	7.568	132.1
Limoptera sp.								
U of A, P906 Lim. 1	0.708201 (14)	1571	1.844	0.0000	542.3	0.19	5.948	168.1
U of A, P906 Lim. 2	0.709501 (09)	1334	1.578	0.0005	633.7	0.19	5.090	196.5
U of A, P906 Lim. 3	0.708628 (14)	1710	2.002	0.0002	499.5	0.19	6.458	154.8
U of A, P906 Lim. 4	0.708505 (10)	1737	1.947	0.0002	513.6	0.19	6.281	159.2
U of A, P906 Lim. 5	0.710979 (10)	1179	1.451	0.0004	689.2	0.19	4.681	213.6
U of A, P906 Lim. 6	0.709192 (12)	1514	1.696	0.0006	589.5	0.19	5.472	182.8
U of A, P906 Lim. 7	0.713105 (09)	726	0.862	0.0007	1160.3	0.19	2.780	359.7
U of A, P906 Lim. 8	0.710099 (08)	1361	1.606	0.0056	622.6	0.19	5.181	193.0
Ibbett Bay								
Atrypa sp.								
TMP 1987.174.2	0.708035 (16)	561	0.681	0.0005	1468.8	0.06	2.196	455.3
II. Hecla Bay Formation								
Ibbett Bay								
Montanaria sp.								
TMP 87.171.02-1	0.709845 (15)	1436	1.720	0.0018	581.4	0.20	5.548	180.2
TMP 87.171.02-2	0.709440 (12)	1094	1.493	0.0000	669.9	0.20	4.815	207.7
TMP 87.171.02-3	0.709957 (09)	1302	1.368	0.0017	731.0	0.20	4.413	226.6
TMP 87.171.02-4	0.709946 (11)	681	0.844	0.0005	1184.2	0.20	2.724	367.1
Montanaria sp.								
GSC C-140085-1	0.709343 (20)	1049	1.407	0.0004	710.6	0.19	4.540	220.3
GSC C-140085-2	0.709969 (24)	3389	1.337	0.0036	747.9	0.19	4.313	231.8
GSC C-140085-3	0.709503 (22)	1052	1.258		794.8	0.19	4.059	246.4
GSC C-140085-4	0.709367 (10)	1532	1.789	0.0004	559.1	0.19	5.770	173.3
Diagenetic calcite								
milled from TMP 87.171.02-3	0.710707 (13)	739	0.728	0.0000	1373.9	0.15	4.852	206.1

* uncertainty, indicated in parentheses, is on the last two decimal places (2σ mean)

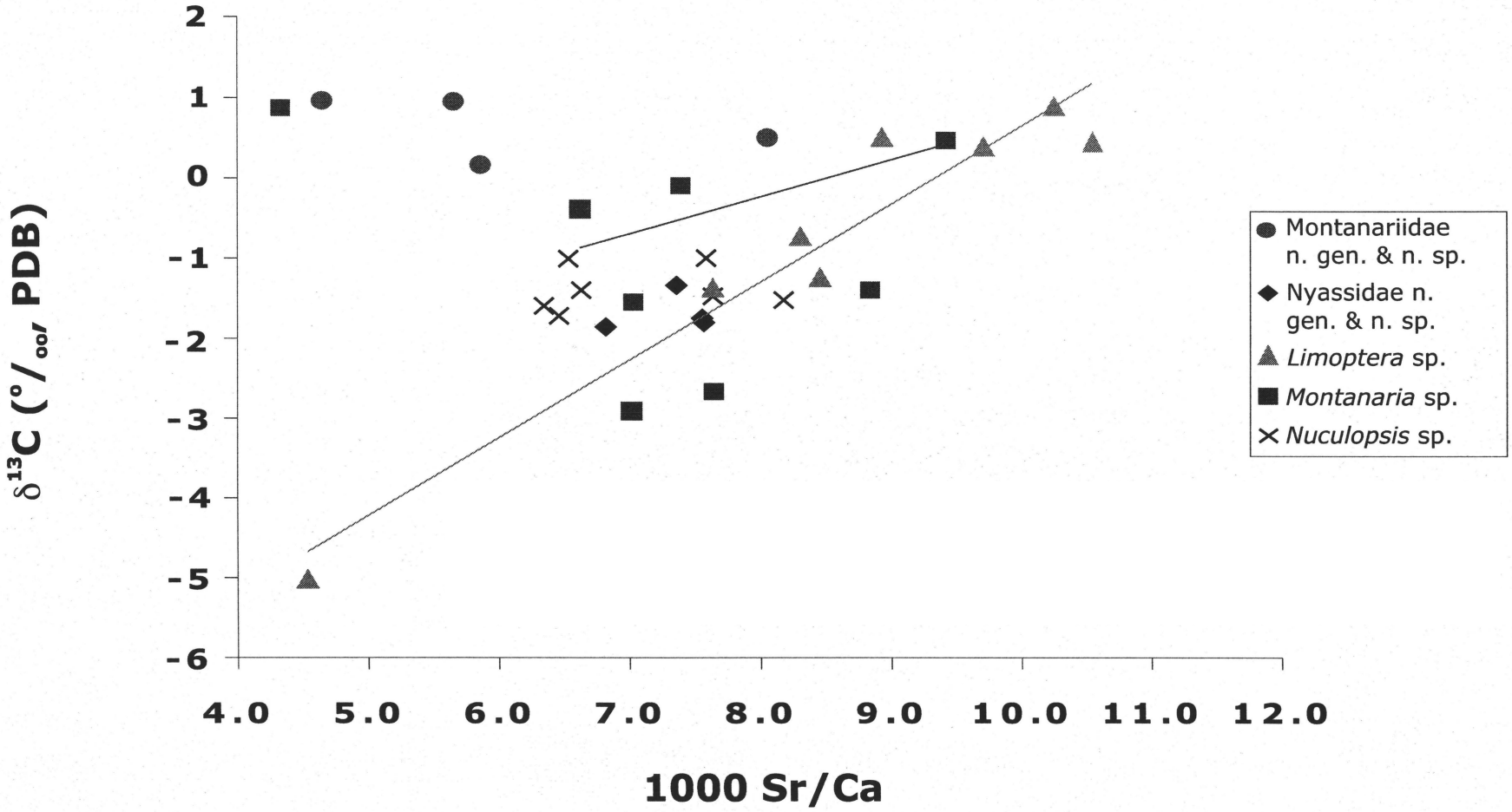

Figure 4-8. $\delta^{13}C$ (PDB) and 1000 Sr/Ca values for carbonate fossils from the Weatherall and Hecla Bay formations. As environmental effects and diagenetic disturbance can produce similar data trends, shell values are difficult to interpret.

water/rock conditions (solid-state recrystallization to calcite) it is expected that the $^{87}Sr/^{86}Sr$ and Sr/Ca ratios of the original water be retained. If, however, substantial fluid is present during neomorphism, when Sr is released from the lattice, it may mix with Sr from pore fluids such that the Sr incorporated into the diagenetic calcite may have an isotopic composition different from that of the original fossil. Because the handsamples chosen for this study consist of siliciclastic lithologies with very little to no carbonate cement, the source of Sr in pore waters will be dominated by the weathering of silicate minerals, and pore-fluid Sr will, therefore, be very radiogenic. Likely, the pore-fluid $^{87}Sr/^{86}Sr$ value will be similar to that characterizing rivers draining the hinterland which, from analyses, is fairly radiogenic and close to the average $^{87}Sr/^{86}Sr$ value of 0.7119 for world rivers. The high Ca/Sr ratio of pore-fluids and their radiogenic composition is confirmed by analysis of calcite spar contained within *Montanaria* sp. (TMP 87.171.02-3), which yielded a $87Sr/^{86}Sr$ value of 0.7107 and a Ca/Sr value of 1374 (1000 Sr/Ca = 0.73).

When $^{87}Sr/^{86}Sr$ values for the carbonate fossils of the Weatherall and Hecla Bay formations (Table 4-4) are plotted against Ca/Sr (Figure 4-9), three major trends are apparent.

Nuculopsis sp., Montanariidae n. gen. & n. sp., and Nyassidae n. gen. & n. sp. (Trend α) show steep trends with high positive slopes, as does *Limoptera* sp. (Trend β), which has broadly the same slope but is offset toward higher Ca/Sr (lower y-intercept).

Montanaria sp. from the interdistributary bay environment of the Hecla bay Formation shows a very different, shallower, $^{87}Sr/^{86}Sr$ – Ca/Sr trend (Trend χ).

The offset in Ca/Sr between the steeply sloping α and β trends most likely reflects

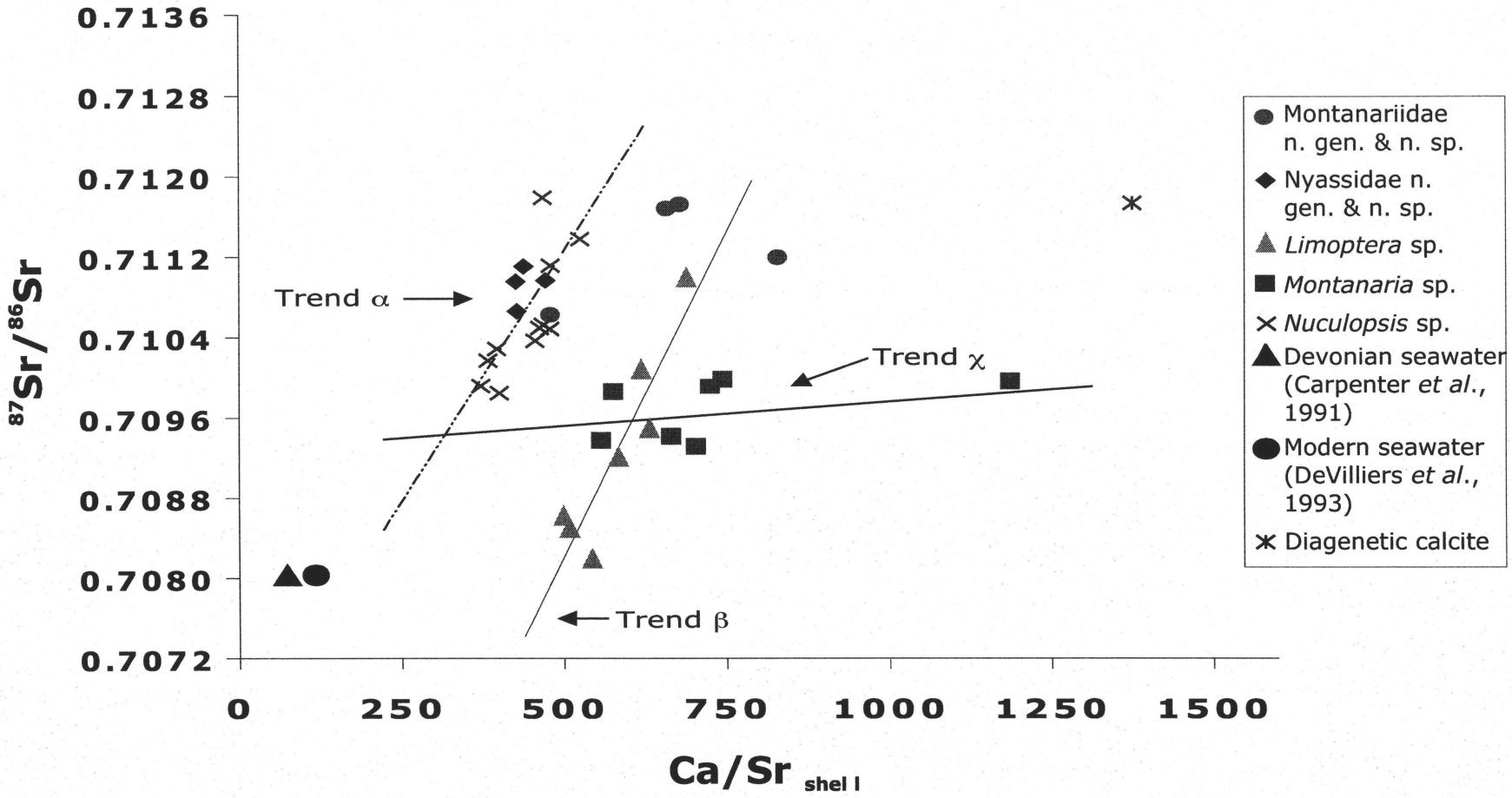

Figure 4-9. $^{87}Sr/^{86}Sr$ vs. shell Ca/Sr data for carbonate fossils of the Weatherall and Hecla Bay formations, showing two steeply sloping D_{Sr} trends (α and β) as well as a shallow trend χ. Most probably, the $^{87}Sr/^{86}Sr$ range of the depositional waters, averaged for all the facies studied, fell between 0.7087 and 0.7096 (Range A) for the mollusks studied, while some *Limoptera* sp. flourished in slightly more seawater influenced brackish environments between 0.7082 and 0.7086 (Range B).

different D_{Sr} values, as the two trends can be brought into alignment on a $^{87}Sr/^{86}Sr$ – Ca/Sr_{water} diagram using biologically reasonable species-specific D_{Sr} values. The fact that the vital effect on D_{Sr} appears to be preserved opens up the possibility that the steeply sloping trends, in particular, may not be entirely a consequence of Sr exchange during neomorphism.

Additionally, post-depositional diagenesis would be expected to homogenise Sr concentrations, regardless of species. The fact that this is not observed in specimens of *Limoptera* sp. and Nyassidae n. gen. & n. sp., collected from the same hand sample, further supports the premise of solid-state neomorphism and preservation of nominal environmental signatures.

Limoptera sp. occurs over a range of facies, from the base of the source distal shelf area to the top of the delta marginal environment (Goodbody, unpublished data; 1987). As they are taken from storm lag deposits (Johnston and Goodbody, 1988), handsamples may contain individual specimens from a variety of environments within the brackish water depositional system. Thus, as *Limoptera* sp. is found in the same handsample as Nyassidae n. gen. & n. sp., post-depositional diagenesis, which would, presumably, influence all shells in the handsample to a similar degree, regardless of species, may not be fully responsible for the trend lines.

In contrast to trends α and β, the shallow sloping *Montanaria* sp. line (Trend χ) suggests a greater degree of Sr loss and higher water/rock ratios during neomorphism.

Continuing with the conservative view that these are diagenetic trends, the least altered values likely lie at the base of the trend lines, toward lower $^{87}Sr/^{86}Sr$ and Ca/Sr ratios. Accordingly, samples U of A P906-1, P906-3, P906-4, and GSC C-140085-4, which lie at the base of these trends, show generally good preservation based on trace element

geochemistry, with relatively low Fe, Mn and Mg concentrations and high Sr content (Table 4-2).

Back-extrapolation of the trend lines to their least diagenetically altered ends reveals that they converge in the $^{87}Sr/^{86}Sr$ range between 0.7087 and 0.7010 (Range A), with some relatively well-preserved *Limoptera* sp. occupying a second range between 0.7082 and 0.7086 (Range B). This suggests that the range of $^{87}Sr/^{86}Sr$ that characterised the depositional waters of the Melville Island mollusks, averaged for all the facies studied, fell between 0.7087 and 0.7010, while some *Limoptera* sp. flourished in slightly more seawater influenced brackish environments.

Rather than considering all the specimens sampled, further discussion of isotope data will be limited to specimens that fall in these ranges (A & B). Handling the data in this fashion enhances the likelihood that genuine paleoenvironmental signatures have been extracted from the shell data, but does not greatly diminish the interpretations that can be made with respect to the nature of the depositional environment and paleosalinity.

4.2.2 Paleosalinity estimation using Sr and O paleohydrology

4.2.2.1 Sr isotope paleohydrology

Atrypa sp. (TMP# 1987.174.2), from the base of the Weatherall Formation, was used to define the marine endmember, as it yielded a Sr/Ca ratio (Table 4-4) comparable to those of fully marine brachiopods (Lowenstam, 1961; Thompson & Chow, 1955). This specimen exhibited a $^{87}Sr/^{86}Sr$ of 0.708035 (Table 4-4), consistent with the findings of Veizer, *et al.* (1999), who determined that the $^{87}Sr/^{86}Sr$ ratio of seawater ranged from 0.7079 in the Late Givetian to 0.7081 in the Early Frasnian.

The Sr freshwater endmember was determined based on an analysis of world river data by Holmden *et al.* (1997). According to this analysis, a $^{87}Sr/^{86}Sr$ ratio of 0.7119 and a Sr

concentration of 0.071 ppm represent median (50th percentile) values for a freshwater environment.

Given the $^{87}Sr/^{86}Sr$ ratios and Sr concentrations of contemporaneous marine and riverine endmembers, two-component mixing curves can be constructed and paleosalinities calculated. The three curves displayed in Figure 2-7 provide a means of gauging the potential uncertainty in the calculated salinity values, which results from a lack of knowledge of the Sr concentration in the freshwater endmember. Salinity ranges are determined based on the two curves bounding the median. The median curve is plotted using 50th percentile values for the Sr concentration and $^{87}Sr/^{86}Sr$ ratio in world rivers and lakes, while the bounding curves are plotted using 20th and 80th percentile values, respectively. The principal assumption is that the observed variance of $^{87}Sr/^{86}Sr$ ratios in the shells is a consequence of two-component mixing between Devonian seawater and freshwater.

In Figure 4-10, the ranges derived from Figure 4-9 are incorporated into the $^{87}Sr/^{86}Sr$ mixing hyperbolae. Paleosalinities based on molluskan $^{87}Sr/^{86}Sr$ ratios from Range A (0.7087 – 0.7010) and Range B (0.7082 – 0.7086) are shaded between mixing hyperbolae that represent near maximum (upper hyperbola) and minimum (lower hyperbola) paleosalinities. This technique of paleosalinity calculation yields a salinity range of 0 $^{o}/_{oo}$ to 5 $^{o}/_{oo}$, for the majority of specimens, with *Limoptera* sp. inhabiting waters of up to 14 $^{o}/_{oo}$.

4.2.2.2 O isotope paleohydrology

Although the oxygen isotope composition of brackish waters, formed by seawater – freshwater mixing, is subject to non-conservative mixing effects due to evaporation, if the residence time for mixed waters is low, or the environment humid, paleosalinities

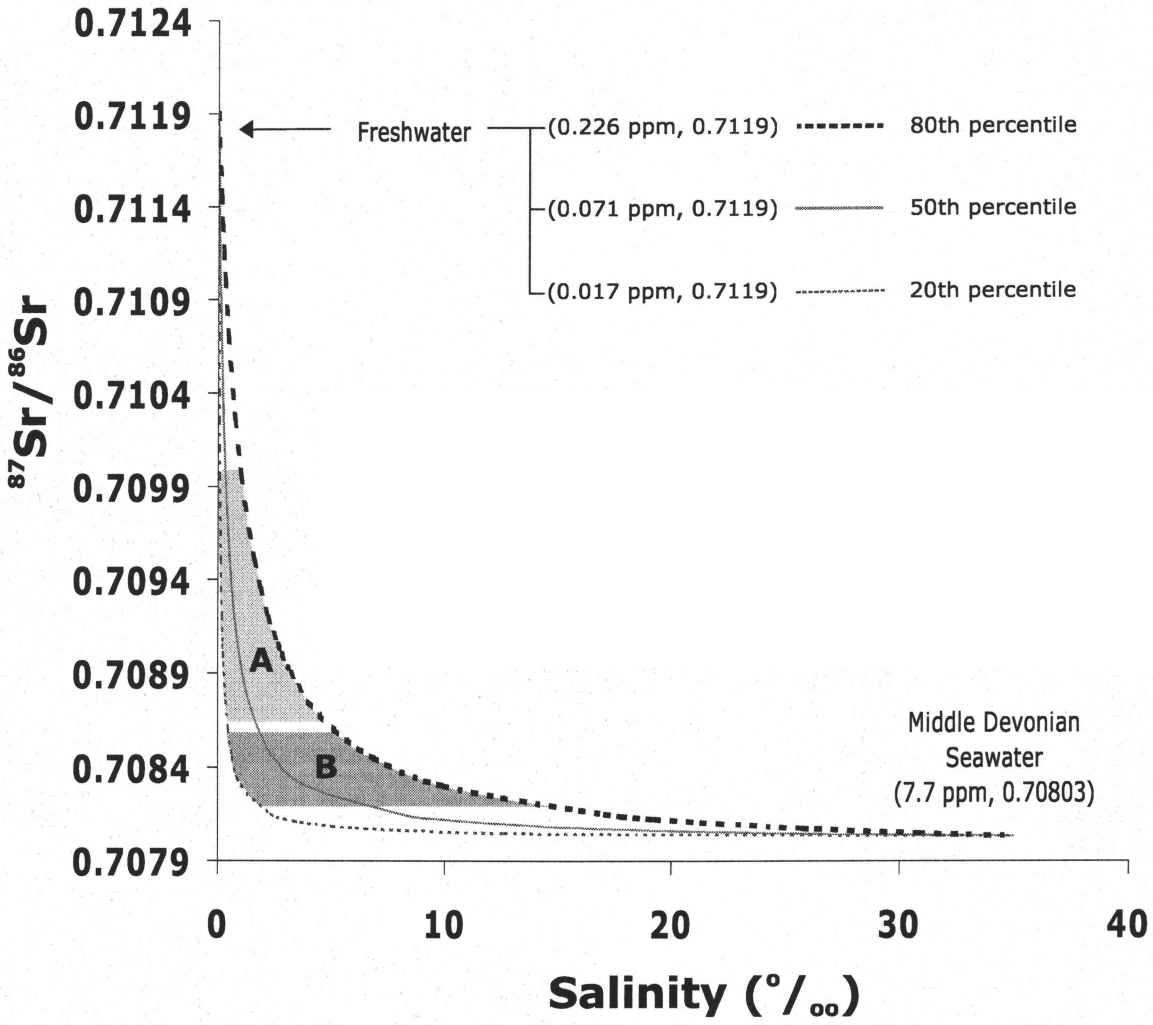

Figure 4-10. Two-component mixing curves for the Middle Devonian of Melville Island based on $^{87}Sr/^{86}Sr$ paleohydrology. The $^{87}Sr/^{86}Sr$ freshwater endmember is determined using mean world river data from Holmden *et al.* (1997). The $^{87}Sr/^{86}Sr$ seawater endmember is determined using *Atrypa* sp. (TMP# 1987.174.2) from the base of the Weatherall Formation, this study. The solid curve is constructed with these seawater and freshwater endmembers and the median (50th percentile) values for the Sr concentration of freshwater in world rivers and lakes. The dashed curves are plotted using 20th and 80th percentile values, respectively. The ranges derived from Figure 4-9 are incorporated into the $^{87}Sr/^{86}Sr$ mixing hyperbolae. This technique of paleosalinity calculation yields a minimum salinity range of 0 °/$_{oo}$ to 5 °/$_{oo}$ for the majority of specimens (shaded zone A), with *Limoptera* sp. inhabiting waters of up to 14 °/$_{oo}$ (shaded zone B).

determined from the O isotope balance in brackish waters should be equal to, or slightly greater than, the Sr isotope paleosalinities (Holmden *et al.*, 1997; Hendry *et al.*, 1997). The specimen of *Atrypa* sp. from the base of the Weatherall Formation, used as the marine endmember for the $^{87}Sr/^{86}Sr$ method, displayed a $\delta^{18}O$ value of –4.9 $^{o}/_{oo}$ (PDB) (Table 4-3), consistent with the findings of Carpenter *et al.* (1991) for abiotic marine cements in Devonian carbonates from Alberta.

Samples of *Montanaria* sp. (GSC C-140085 and TMP 87.171.02) from the mono-specific shell beds of the Hecla Bay Formation yielded the lowest shell $\delta^{18}O$ values of the studied specimens, clustering between –8 $^{o}/_{oo}$ and –13 $^{o}/_{oo}$ (PDB) (Table 4-3).

The temperature dependent carbonate-water equilibrium fractionation equation of O'Neil *et al.* (1969) was employed to convert $\delta^{18}O_{carbonate}$ values to $\delta^{18}O_{water}$ values;

$$1000 \ln \alpha = \frac{2780000}{T^2} - 3.39 \qquad (4.1)$$

where

$$\alpha = \frac{\delta^{18}O_{carb} + 1000}{\delta^{18}O_{water} + 1000} \qquad (4.2)$$

As the study site is believed to have been located in the tropical equatorial region (Ziegler, 1988; Scotese and McKerrow, 1990; Scotese, 2000), as discussed in section 4.1.3, early Cenozoic and modern equatorial sea surface temperatures can be utilized to estimate a paleotemperature range for the depositional waters of the Weatherall and Hecla Bay formations. Based on the determined average seasonal temperature range (24° C to 28° C), an average paleotemperature of 26° C was employed to determine $\delta^{18}O_{water}$ values from measured $\delta^{18}O_{carbonate}$ values (Table 4-3).

Application of the carbonate-water equilibrium fractionation equation yields a $\delta^{18}O$ value of –2.28 ‰ (SMOW) for the seawater endmember. For the freshwater endmember, two compositions determined from $\delta^{18}O_{carbonate}$ values of -13.1 ‰ (PDB) and –11.1 ‰ (PDB) (the specimen with the most negative $\delta^{18}O$ value, TMP 87.171.02-2, and the best-preserved *Montanaria* sp. specimen, based on trace element geochemistry, GSC C-140085-4), which yield $\delta^{18}O_{water}$ values of -10.40 ‰ (SMOW) and –8.39 ‰ (SMOW) at 26° C, are used. Two O isotope mixing lines were generated using these values, to highlight the uncertainty on paleosalinities as a result of the freshwater endmember selection (Figure 4-11).

Modern meteoric water from equatorial coastal stations has a $\delta^{18}O$ range of 0 ‰ to –2 ‰ (Yurstsever & Gat, 1981). The lower $\delta^{18}O$ value for Melville Island in the Devonian can be attributed to an orographic effect on the O isotope composition of precipitation caused by the nearby Ellesmerian Mountains (Holmden *et al.*, 1997).

As with the $^{87}Sr/^{86}Sr$ ratio method, the principal assumption, using this technique of paleosalinity determination, is that of two-component mixing; that the O isotope systematics and salinity of the Weatherall and Hecla Bay depositional waters were controlled by mixing between seawater and freshwater.

One specimen from each species was plotted on Figure 4-11 based on geochemical preservation; only samples with low Fe, Mn and Mg, as well as high Sr (Table 4-3) were selected. The $\delta^{18}O$ values for the selected Melville Island mollusks (Table 4-3) define a range of salinity from 0 ‰ to 19 ‰ using a riverine endmember of –10.40 ‰, and a salinity range of 0 ‰ to 14 ‰ using a freshwater endmember of –8.39 ‰. While this is broadly consistent with the salinity range of 0 ‰ to 14 ‰ calculated using Sr isotope

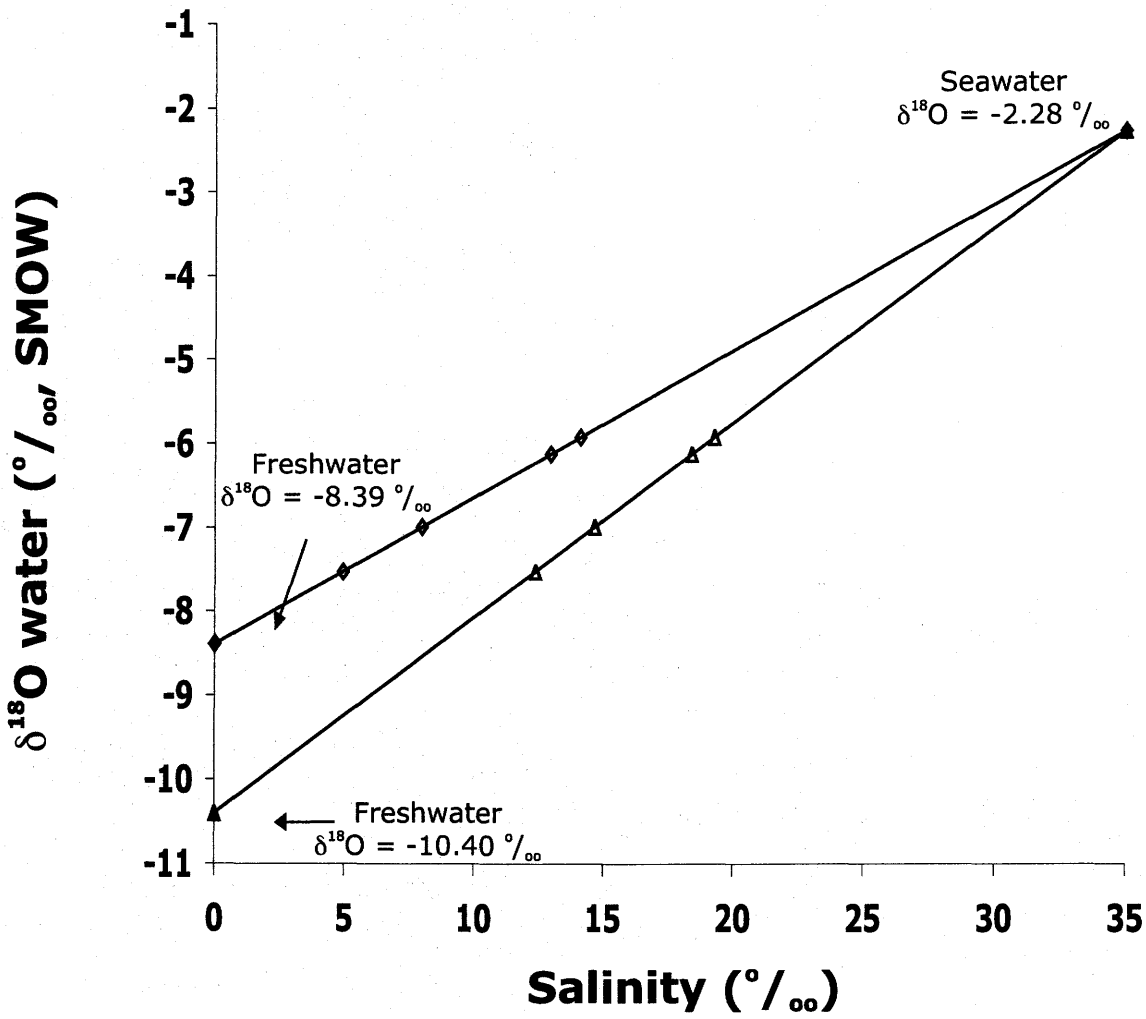

Figure 4-11. Potential salinity of depositional waters of the Weatherall and Hecla Bay formations. Mollusk $\delta^{18}O$ values were transformed to $\delta^{18}O$ values for the depositional waters assuming an average paleotemperature of 26°C, and using the carbonate-water equilibrium fractionation relationship of O'Neil (1969).). The seawater endmember is based on brachiopod data (TMP 1987.174.2, this study). The freshwater endmembers are determined based on analyses of mollusk specimens (*Montanaria* sp. TMP 87.171.02, this study. Selected samples are plotted on the line and yield a salinity range of 0 °/oo to 14 °/oo for a freshwater endmember of -8.39 °/oo, and a salinity range of 0 °/oo to 19 °/oo for a freshwater endmember of -10.40 °/oo

paleohydrology, only certain specimens of *Limoptera* sp. (U of A P906 Lim 3 and Lim 4) yield similar salinity values using the two different methods (Figure 4-12). As these two specimens lie at the base of Trend β (Figure 4-9) this overlap is likely the result of relatively good preservation of O and Sr isotope signatures in these samples. *Nuculopsis* sp., Nyassidae n. gen. & n. sp., and Montanariidae n. gen. & n. sp. show an offset of up to 14 $^{o}/_{oo}$ between the two techniques, indicating evaporative enrichment of ^{18}O in the mixing zone, or potential diagenetic influence on the $^{87}Sr/^{86}Sr$ ratios.

It must be recognised that, while variability is created by uncertainty on both the paleolatitude and the paleotemperature, a temperature variation of up to 8° C yields a very small salinity variation of ± 2.6 $^{o}/_{oo}$ on inferred paleosalinities.

4.2.3 Sr/Ca ratio of Devonian seawater

In order to calculate the Sr/Ca ratio of the depositional waters, shell Sr/Ca values are transformed to water Sr/Ca values using biologically reasonable species-specific D_{Sr} values (Table 4-4) and plotted against $^{87}Sr/^{86}Sr$. D_{Sr} values between 0.19 and 0.33 (Table 4-4) were used, which span the range of observed D_{Sr} in modern freshwater, aragonitic mollusks (Odum, 1951; Faure *et al.*, 1967; Buchardt & Fritz, 1978; Rosenthal & Katz, 1989). When the same D_{Sr} is applied to both of the steeply sloping trends in Figure 4-9 (α and β), both shift an equal distance to the left. Thus, if a D_{Sr} of 0.33 is applied to both groups, they both shift equally toward lower Ca/Sr ratios (higher Sr/Ca). The same is true if a D_{Sr} of 0.19 is applied, although the translation distance is greater. If, however, a D_{Sr} of 0.33 is applied to one group and a D_{Sr} of 0.19 is applied to the other, reflecting different species-specific D_{Sr}, the two trends can be made to overlap (Figure 4-13). Thus, by judicious application of biologically reasonable D_{Sr} values, the shell Ca/Sr

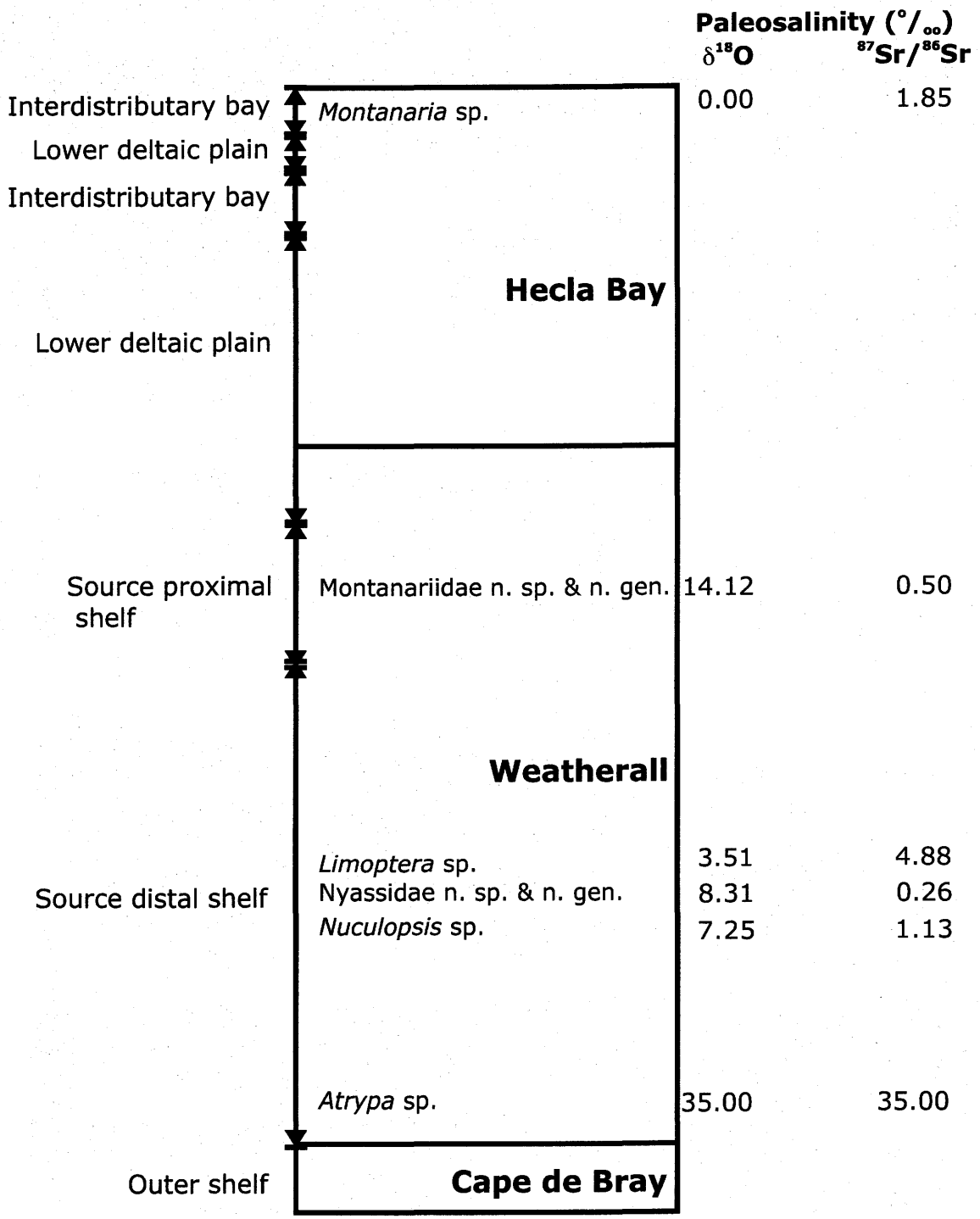

Figure 4-12. Schematic stratigraphic column showing vertical facies relationships and approximate locations of sampled species. Inferred paleosalinities based on Sr isotope (80th percentile data) and $\delta^{18}O$ (freshwater endmember of -8.39 °/oo) calculations for samples GSC C-140085-4, TMP 87.162.3-3, U of A P906 Lim 3, U of A P906 Cyc 2, TMP 187.162.1-7, and TMP 1987.174.2 are also shown.

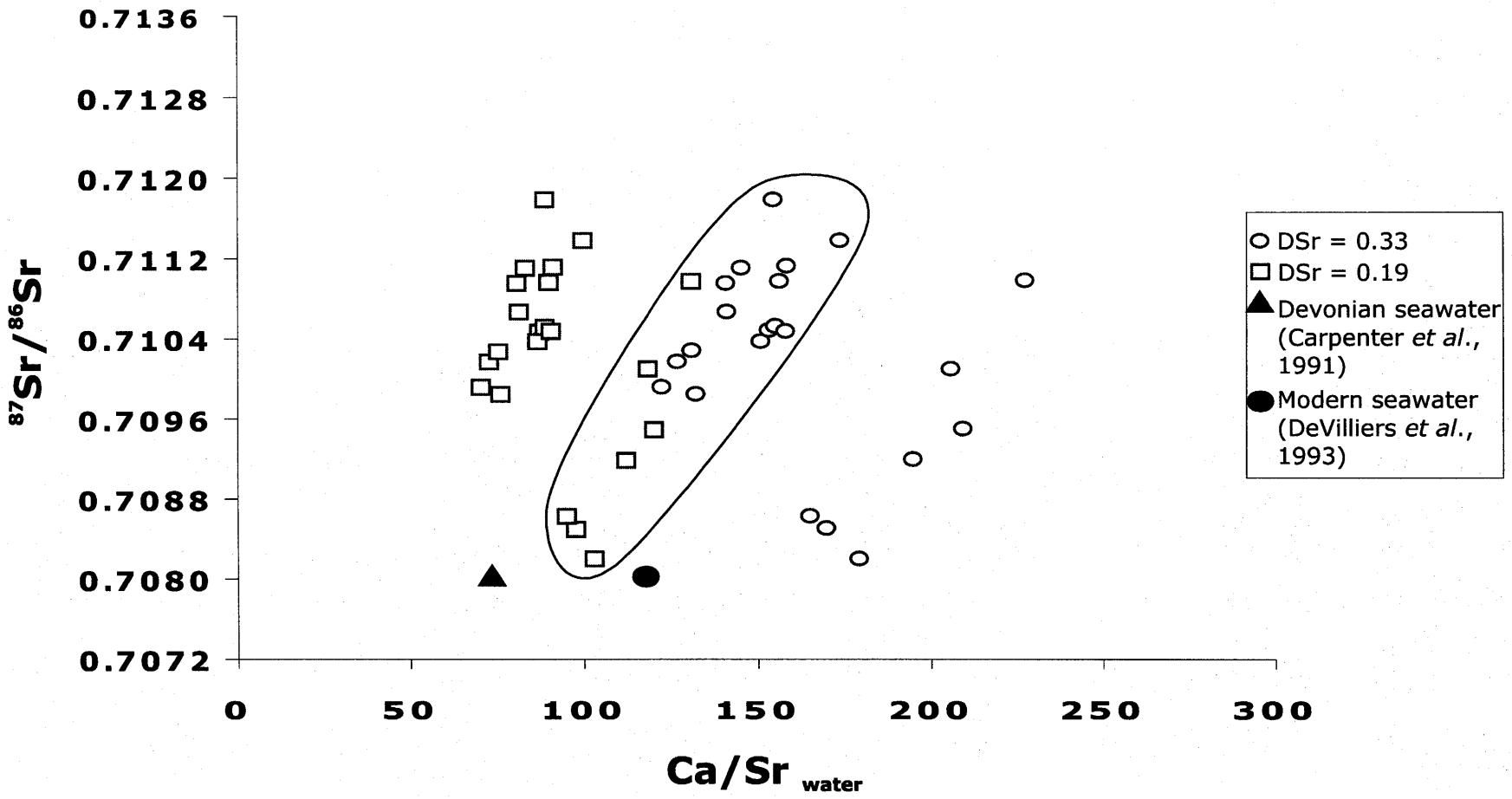

Figure 4-13. $^{87}Sr/^{86}Sr$ vs. water Ca/Sr data for carbonate fossils of the Weatherall and Hecla Bay formations showing trend variation with D_{Sr}. If a D_{Sr} of 0.33 is applied to one group and a D_{Sr} of 0.19 is applied to the other, the two can be made to overlap.

data (trends α, β and χ) are transformed to equivalent water Ca/Sr ratios, and the data brought into alignment. The result is a broad, steeply sloping data array on the $^{87}Sr/^{86}Sr$ – Ca/Sr diagram.

In the analysis of the $^{87}Sr/^{86}Sr$ – Ca/Sr data, it was conservatively concluded that the trends displayed by fossil specimens from individual hand samples were diagenetic trends. The possibility that the steeply sloping $^{87}Sr/^{86}Sr$ and Ca/Sr trends, in particular, may be genuinely characteristic of the Devonian seawater – freshwater mixing zone, will now be explored. If this were the case, a linear regression through this trend should intersect the $^{87}Sr/^{86}Sr$ and Ca/Sr ratios of Devonian seawater. Thus, using the seawater $^{87}Sr/^{86}Sr$ ratio of 0.70803 (constrained through analysis of *Atrypa* sp.) and a best-fit line generated through linear regression, the Sr/Ca ratio of Devonian seawater can be determined.

The best-fit line is shown in Figure 4-14 and yields a Sr/Ca ratio for Devonian seawater of approximately 14. This is not too different from the modern value of 8.5 (DeVilliers *et al.*, 1993) and provides increased confidence that the steeply sloping trends may not be entirely artifacts of Sr exchange accompanying diagenesis. Indeed, the determined value of 14 is nearly identical to the value of 13.6 obtained for Devonian seawater using marine cement of the Leduc Formation of Alberta (Carpenter *et al.*, 1991). It is emphasized that the estimate of the Sr/Ca ratio for Devonian seawater is dependent upon the slope of the data array. Admittedly, the uncertainty on the slope of the best-fit line is quite large due to the broadness of the data array along the Ca/Sr axis. This reflects either several trend lines of similar slope through the data that reflect slightly different endmember $^{87}Sr/^{86}Sr$ – Ca/Sr composition, or broadening of the shell data due to neomorphic loss of Sr. With respect to the latter explanation, so long as the slope of the

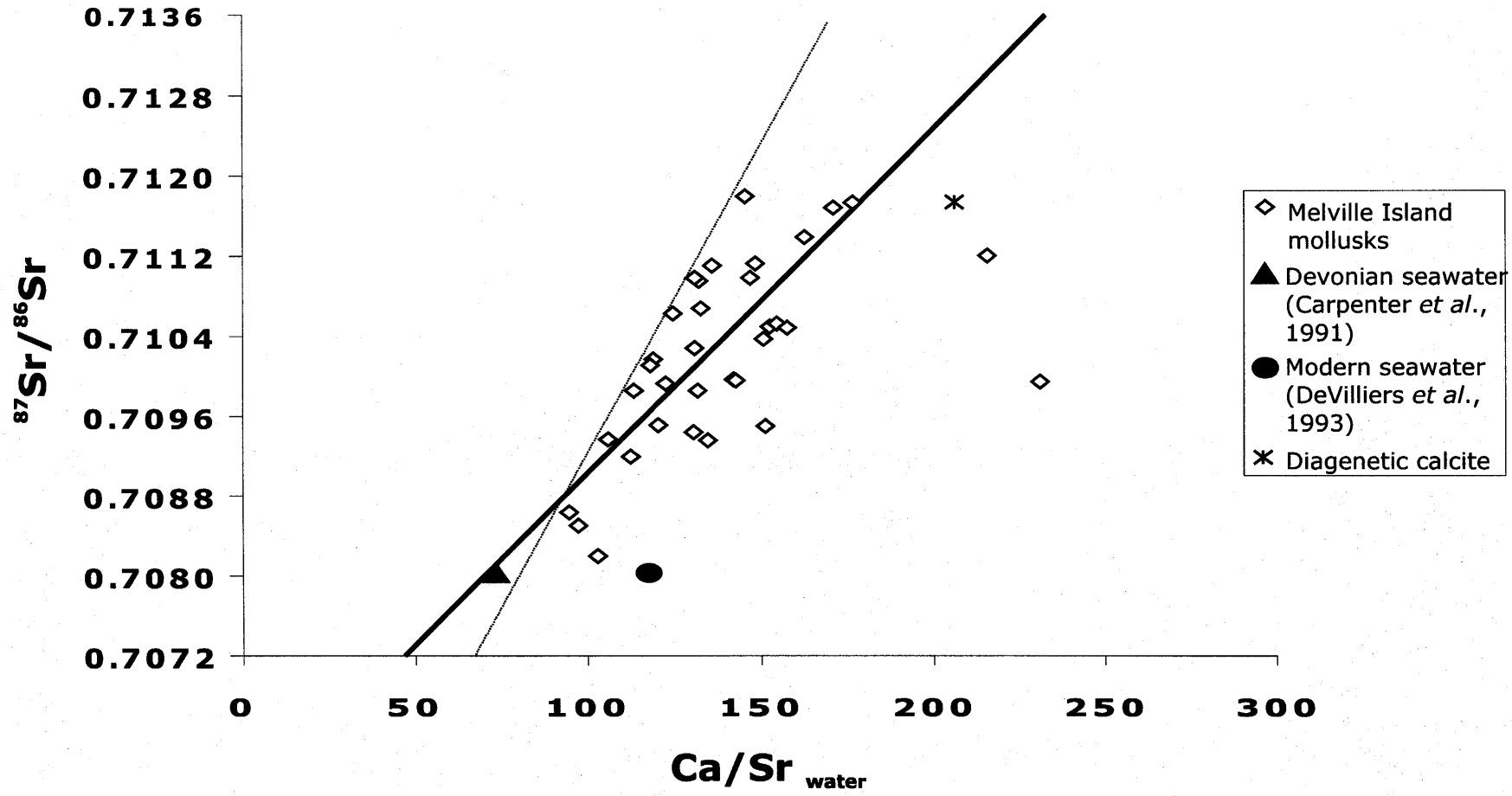

Figure 4-14. $^{87}Sr/^{86}Sr$ vs. water Ca/Sr data for carbonate fossils of the Weatherall and Hecla Bay formations. The species are plotted together to generate a trend line (solid line), which intercepts the $^{87}Sr/^{86}Sr$ value for Devonian seawater at 14.0. Alternately, if the trend line is drawn on the low Ca/Sr side of the data (dashed line), i.e. the area of minimum diagenetic alteration, Devonian seawater is intersected at 12.5. The fact that partially recrystallized Devonian fossils plot on a line that intersects seawater at a reasonable value gives strong evidence for two-component mixing. Samples TMP 87.171.02-4 and TMP 87.162.3-1 were not included in the calculations, as both show very high Sr loss as a result of relatively severe diagenesis.

original water composition is unchanged by neomorphism, the Sr/Ca of Devonian seawater can still be estimated. Therefore, assuming that some loss of Sr has shifted the inferred water compositions to the right on Figure 4-14, a line is fit to the extreme left side of the data array (the high Sr side). This line, shown in Figure 4-14, yields a Sr/Ca ratio of 12.5 for a Devonian marine $^{87}Sr/^{86}Sr$ ratio of 0.70803.

It is difficult to estimate the uncertainty on the Sr/Ca ratio. One source of uncertainty is the choice of D_{Sr} necessary to transform the Ca/Sr shell data to equivalent Ca/Sr water data. In this case, however, the potential uncertainty is minimised because the D_{Sr} values used to bring trends α and β into alignment span the known range of D_{Sr} for modern aragonitic mollusks. Thus, any other choice of D_{Sr} would not provide the observed alignment while satisfying the criterion of being biologically reasonable. The main uncertainty, therefore, is the slope of the line through the data array. Given the large uncertainty on the slope of the best-fit line, the Sr/Ca ratio obtained using the line fit to the high Sr side of the data can be considered more justifiable.

The Sr/Ca ratio inferred for Devonian seawater, higher than the modern value of 8.5 (DeVilliers *et al.*, 1993), may be partially attributable to the great extent of calcite precipitation during the Palaeozoic (Wilkinson *et al.*, 1985; Sandberg, 1985). Carpenter *et al.* (1991) also propose that the decrease in the $^{87}Sr/^{86}Sr$ ratios of marine carbonates toward the end of the Devonian (Burke *et al.*, 1982) may be the result of increased hydrothermal vent flux from oceanic crust which, when combined with riverine influx and marine carbonate precipitation, could increase the Sr/Ca ratio of seawater (Palmer & Edmond, 1989).

In summary, the inferred Sr/Ca ratio for Devonian seawater is reasonable and consistent with previous estimates, which provides increased confidence in the $^{87}Sr/^{86}Sr$ paleosalinity results based on the assumption of seawater – freshwater mixing.

5.0 DEPOSITIONAL ENVIRONMENT

Bivalves from the Weatherall Formation are constrained by their Sr and O isotope paleohydrologies to have been deposited in a marginal marine setting. Paleosalinities inferred from these two methods are broadly consistent, yielding values between 0 $^{o}/_{oo}$ and 19 $^{o}/_{oo}$. This interpretation conforms with sedimentological studies of the area, which suggest a deltaic environment of deposition, shown by the coarsening-upward sequences of the Weatherall Formation on eastern Melville Island (Goodbody, 1988; Goodbody, 1994). It also conforms with the vertical distribution of the mollusk fossils within the strata, as salinity values calculated from the fossil mollusks increases with sediment depth and, therefore, marine influence; based on $^{87}Sr/^{86}Sr$ paleosalinity calculations. Samples from the source distal environment of the Weatherall Formation yielded salinity values of up to 14 $^{o}/_{oo}$, while samples from the overlying source proximal and interdistributary bay deposits yielded up to 2 $^{o}/_{oo}$ salinity. This confirms that the bivalve-dominated assemblages of the Weatherall and Hecla Bay formations were deposited in waters of reduced salinity.

High volumes of freshwater, flowing from the Ellesmerian highlands into the shallow marine waters on the epicontinental platform, would result in a very extensive freshwater jet. As Melville Island was located near the northwest margin of the continental plate in the Middle Devonian (Ziegler, 1988), freshwater was discharged slopeward, into the shallow marine waters overlying the continental shelf. High-volume riverine discharge onto the shelf could explain the large geographic extent of the

Weatherall and Hecla Bay formations, as the shallow waters of the continental platform would lead to a laterally extensive zone of mixed waters (Figure 5-1) and a low seaward salinity gradient (Bates, 1953).

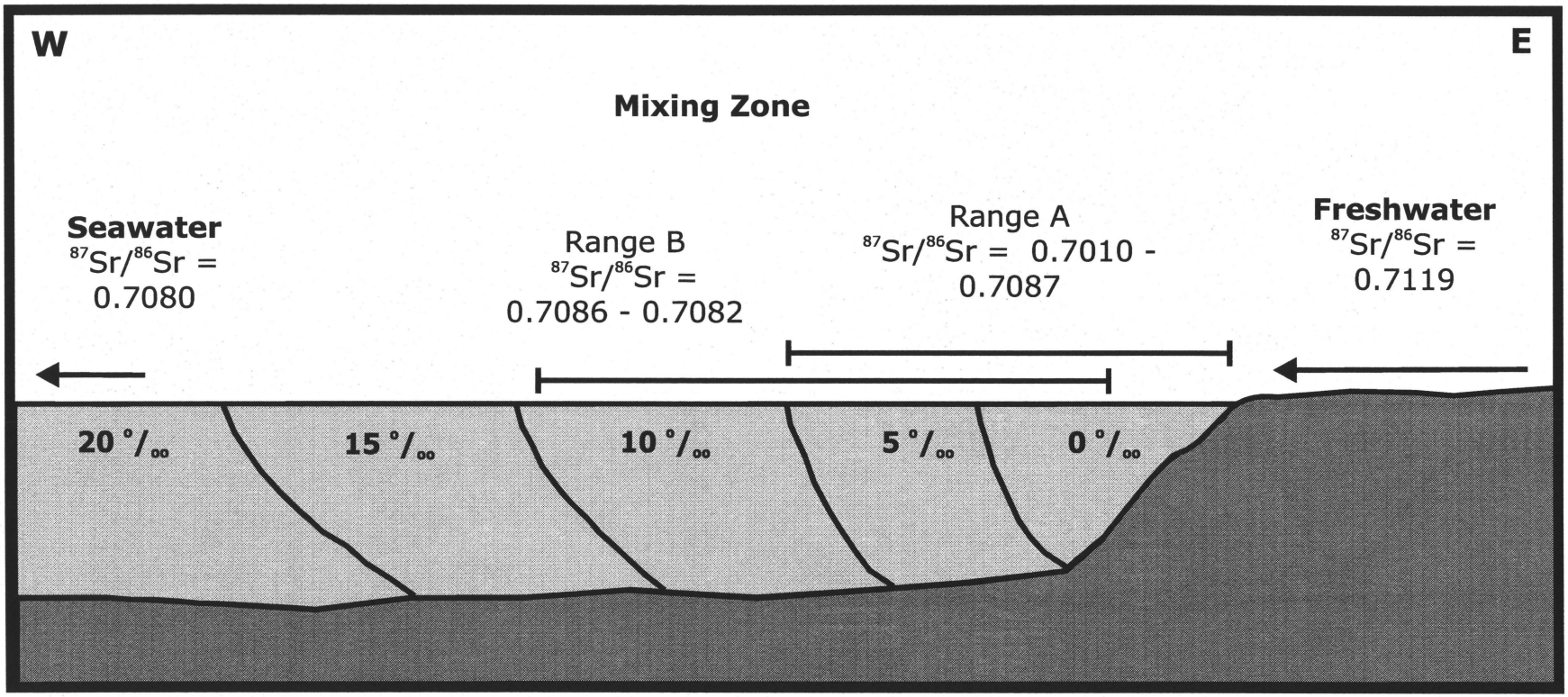

Figure 5-1. Stylized cross-section of the depositional environments of the carbonate fossils of the Weatherall and Hecla Bay formations, showing $^{87}Sr/^{86}Sr$ values for freshwater and seawater. $^{87}Sr/^{86}Sr$ Range A, averaged for all the facies studied, corresponds with the mixing zone between these two endmembers and is also shown. Salinity is given in per mil. High volumes of freshwater, flowing from the Ellesmerian highlands into the shallow marine waters overlying the continent-facing deltaic shelf, would result in a very extensive freshwater lens which, in turn, would inhibit vertical salinity stratification in the water column, leading to a laterally extensive zone of mixed waters and a low seaward salinity gradient (Bates, 1953).

6.0 CONCLUSIONS

Sr, O and C isotopic measurements of fossil shells of Devonian bivalves species *Limoptera* sp., *Nuculopsis* sp., Nyassidae n. gen. & n. sp., Montanariidae n. gen. & n. sp. and *Montanaria* sp. were performed in order to investigate the isotope paleohydrology and environment of an unusual bivalve-dominated marginal marine sequence from the siliciclastic Weatherall and Hecla Bay formations, Melville Island.

Due to the age of these specimens, confirmation that measured chemical and isotopic compositions have not been substantially overprinted by diagenesis was necessary to accurately interpret environmental, chemical and isotopic signatures. To this end, shell microstructure, mineralogy and trace element geochemistry were investigated and considerable evidence amassed in support of the premise that the Devonian mollusks of Melville Island have been transformed from their original aragonite mineralogy to calcite under relatively closed-system diagenesis. XRD analysis indicated that the fossils contain up to 18% relic aragonite, thus far the oldest known preserved aragonite in the rock record, finely disseminated on a millimetre scale within the recrystallized shell. Trace element geochemistry analysis yielded Fe, Mn and Mg concentrations higher than modern aragonite marine bivalves. However, as the Melville Island fossils are thought to have been precipitated within the seawater – freshwater mixing zone, covariant trends in trace elements and isotopes recorded in the shells may actually reflect the original environmental range of elemental and isotopic abundances in the brackish depositional water. Of additional use in extricating potential diagenetic trends from

environmental trends was the $^{87}Sr/^{86}Sr$ – Ca/Sr diagram. With this diagram, it was possible to use trend lines defined by individual species from single handsamples to reverse the potential effects of Sr exchange during aragonite neomorphism. Extrapolation of the fossil trends toward lower Ca/Sr (higher Sr) and lower $^{87}Sr/^{86}Sr$ resulted in convergence of the trend lines within a relatively narrow range of $^{87}Sr/^{86}Sr$ ratios, which is interpreted as the mean $^{87}Sr/^{86}Sr$ for depositional waters of the Weatherall and Hecla Bay formations, averaged over all facies.

Two methods of paleosalinity determination were applied in order to reconstruct the paleosalinity regime of this bivalve dominated assemblage. Under the first, the $^{87}Sr/^{86}Sr$ ratios inferred for the depositional waters of the Weatherall and Hecla Bay formations were used to construct a two-component, seawater-freshwater, mixing hyperbola. Material balance calculations yielded paleosalinities between 0 $^{o}/_{oo}$ and 14 $^{o}/_{oo}$, dependent upon the concentration of Sr chosen for the riverine endmember (20^{th} and 80^{th} percentiles for world rivers), consistent with sedimentological studies of the area, which suggest a deltaic environment of deposition.

The second technique involved the determination of paleosalinities based on the O isotope paleohydrology and $\delta^{18}O$ values of mollusks. Using a riverine endmember of -10.40 $^{o}/_{oo}$ (SMOW), material balance calculations yielded paleosalinities between 0 $^{o}/_{oo}$ and 19 $^{o}/_{oo}$, while a riverine endmember of –8.39 $^{o}/_{oo}$ yielded paleosalinities of 0 $^{o}/_{oo}$ to 14 $^{o}/_{oo}$. While this is broadly consistent with the salinity range inferred from Sr isotope paleohydrology, only certain specimens of *Limoptera* sp. yields similar salinity values using the two different methods. *Nuculopsis* sp., Nyassidae n. gen. & n. sp., and Montanariidae n. gen. & n. sp. show an offset of up to 14 $^{o}/_{oo}$ between the two

techniques, likely due to evaporative enrichment of ^{18}O in the mixing zone or the effects of diagenesis on shell $^{87}Sr/^{86}Sr$.

In addition to determining the salinity of the depositional waters of the Weatherall and Hecla Bay formations, the Sr/Ca ratio of Devonian seawater was graphically determined using selected data on the $^{87}Sr/^{86}Sr - Ca/Sr$ diagram, yielding a 1000Sr/Ca ratio of approximately 12.5. The Sr/Ca ratio inferred for Devonian seawater, higher than the modern value of 8.5 (DeVilliers *et al.*, 1993), may result, in part, from the vast amounts of marine carbonates precipitated during the Paleozoic (Wilkinson *et al.*, 1985; Sandberg, 1985), when sea levels were higher than today. The increase in the Sr/Ca of seawater, when considered with the decrease in $^{87}Sr/^{86}Sr$ at the end of the Devonian (Burke *et al.*, 1982), may also reflect an increase in the hydrothermal vent flux from oceanic crust (Palmer & Edmond, 1989), as the combination of riverine influx, marine carbonate deposition and large scale hydrothermal vent activity could raise the Sr/Ca of seawater.

REFERENCES

Andersson P.S., Wasserburg F.J., and Ingri J. (1992) The sources of Sr and Nd isotopes in the Baltic Sea. *Earth and Planetary Science Letters* **113**, 459-472.

Andreasson F. P. and Schmitz B. (2000) Temperature seasonality in the early middle Eocene North Atlantic region: Evidence from stable isotope profiles of marine gastropod shells. *Geological Society of America Bulletin* **112**(4), 628-640.

Arthur M.A., Williams, D.F. and Jones D.S. (1983) Seasonal temperature-salinity changes and thermocline development in the Mid-Atlantic Bight as recorded by the isotopic composition of bivalves. *Geology* **11**, 655-659.

Barbin V. (2000) Cathodoluminescence of Carbonate Shells: Biochemical vs Diagenetic Processes. In *Cathodoluminescence in Geosciences* (ed. M. Pagel, V. Barbin, P. Blanc, and D. Ohnenstetter), pp. 303-330. Springer Verlag.

Barnes R.S.K. (1989) What, if anything, is a brackish-water fauna? *Transactions of the Royal Society of Edinburgh: Earth Sciences* **80**, 235-240.

Barrell J. (1912) Criteria for the recognition of ancient delta deposits. *Bulletin of the Geological Society of America* **23**, 377-446.

Barwood H.L. (2000) Using NIH-Image to convert powder X-ray diffraction camera films to digital diffractograms. *http://www.indiana.edu/~xl10rd/digiabst.htm*, pp. 1-8.

Bates C.C. (1953) Rational Theory of Delta Formation. *American Association of Petroleum Geology Bulletin* **39**, 2119-2162.

Bøggild O. B. (1930) The shell structure of the mollusks. *Mémoires de l'Académie Royale des Sciences et des Lettres de Danemark* **9**(t. II, no. 2), 235-326.

Brand U. and Veizer J. (1980) Chemical diagenesis of a multicomponent carbonate system; 1, Trace elements. *Journal of Sedimentary Petrology* **50**(4), 1219-1236.

Brand U. (1981) Mineralogy and chemistry of the lower Pennsylvanian Kendrick fauna, eastern Kentucky. *Chemical Geology* **32**, 1-16.

Brand U. (1983) Geochemical analysis of *Nautilus pompilius* from Fiji, South Pacific. *Marine Geology* **53**, M1-M5.

Brand U. (1987) Depositional analysis of the Breathitt Formation's marine horizons, Kentucky, U.S.A.: Trace elements and stable isotopes. *Chemical Geology (Isotope Geoscience Section)* **65**, 117-136.

Brand U. and Morrison J.O. (1987) Paleoscene Biogeochemistry of fossil marine invertebrates. *Geoscience Canada* **14**(2), 85-107.

Brand U., Morrison J.O., Brand N., and Brand E. (1987) Isotopic variation in the shells of Recent marine invertebrates from the Canadian Pacific coast. *Chemical Geology (Isotope Geoscience Section)* **65**, 137-145.

Brand U. (1989) Aragonite-calcite transformation based on Pennsylvanian molluscs; with Suppl. Data 89-06. *Geological Society of America Bulletin* **101**(3), 377-390.

Brand U., Yochelson E.L., and Eagar R.M. (1993) Geochemistry of Late Permian non-marine bivalves: Implications for the continental paleohydrology and paleoclimatology of northwestern China. *Carbonates and Evaporites* **8**(2), 199-212.

Brand U. (1994) Continental hydrology and climatology of the Carboniferous Joggins Formation (lower Cumberland Group) at Joggins, Nova Scotia: evidence from the geochemistry of bivalves. *Palaeogeography, Palaeoclimatology, Palaeoecology* **106**, 307-321.

Buchardt B. and Fritz P. (1978) Strontium uptake in shell aragonite from the freshwater gastropod *Limnaea stagnalis*. *Science* **199**(291-292).

Burke W.H., Denison E.A., Hetherington R.B., Koepnick R.B., Nelson H.F., and Otto J.B. (1982) Variation of seawater $^{87}Sr/^{86}Sr$ ratio throughout Phanerozoic time. *Geology* **10**, 516-519.

Carpenter S.J., Lohmann K.C., Holden P., Walter L.M., Huston T.J., and Halliday A.N. (1991) $\delta^{18}O$ values, $^{87}Sr/^{86}Sr$ and Sr/Mg ratios of Late Devonian abiotic marine calcite: Implications for the composition of ancient seawater. *Geochimica et Cosmochimica Acta* **55**, 1991-2000.

Carter J.G. (1990a) Evolutionary significance of shell microstructure in the Palaeotaxodonta, Pteriomorphia and Isofilibranchia. In *Skeletal Biomineralization: Patterns, Processes and Evolutionary Trends*, Vol. 1 (ed. J.G. Carter), pp. 135-296. Van Nostrand Reinhold.

Carter J.G. (1990b) Shell microstructural data for the Bivalvia. In *Skeletal Biomineralization: Patterns, Processes and Evolutionary Trends*, Vol. 1 (ed. J.G. Carter), pp. 297-391. Van Nostrand Reinhold.

Clarkson E. N. K. (1994) *Invertebrate Palaeontology and Evolution.* Chapman & Hall.

Clayton R. N. and Degens., E.T. (1959) Use of carbon isotope analyses of carbonates for differentiating freshwater and marine sediments. *American Association of Petroleum Geologists Bulletin* **43**, 890-897.

Coleman J.M. (1981) *Deltas: processes of deposition and models for exploration.* Continuing Education Publication Co.

Craig H. (1961) Isotopic variations in meteoric waters. *Science* **133**, 1702-1703.

Davies T.T. and Hooper P.R. (1963) The determination of the calcite - aragonite ratio. *Mineralogical Magazine* **33**, 602-612.

Dennis A.M. & Lawrence D.R. (1979) Macrofauna and fossil preservation in the Magoffin marine zone, Pennsylvanian Breathitt Formation of eastern Kentucky. *Southeastern Geology* **20**, 181-190.

DeVilliers S., Shen G.T., and Nelson B.K. (1993) The Sr/Ca-temperature relationship in coralline aragonite: Influence of variability in $(Sr/Ca)_{seawater}$ and skeletal growth parameters. *Geochimica et Cosmochimica Acta* **58**, 197-208.

Dodd J.R. and Stanton R.J. (1975) Paleosalinities within a Pliocene bay, Rettleman Hills, California: a study of the resolving power of isotope and faunal techniques. *Geological Society of America Bulletin* **86**, 52-64.

Embry A.F. and Klovan J.E. (1976) The Middle-Devonian clastic wedge of the Franklinian Geosyncline. *Bulletin of Canadian Petroleum Geology* **24**(4), 485-639.

Embry A.F. (1988) Middle-Upper Devonian sedimentation in the Canadian Arctic Islands and the Ellesmerian Orogeny. In *Devonian of the World*, Vol. II (ed., N.J. McMillan, A.F. Embry, D.J. Glass), pp. 15-28. Canadian Society of Petroleum Geologists.

Embry A.F. (1991) Middle-Upper Devonian clastic wedge of the Arctic Islands. In *Geology of the Innuitian Orogen and Arctic Platform of Canada and Greenland*, Vol. Geology of Canada, no.3 (ed. H.P. Trettin), pp. 263-279. Geological Survey of Canada.

Epstein S. and Lowenstam H.A. (1953) Temperature-shell-growth relations of recent and interglacial Pleistocene shoal water biota from Bermuda. *J. Geol.* **61**, 424-438.

Faure G., Crocket J.H., and Hurley P.M. (1967) Some aspects of the geochemistry of strontium and calcium in Hudson Bay and the Great Lakes. *Geochimica et Cosmochimica Acta* **31**, 451-461.

Flament P. (1996) The Ocean Atlas of Hawai'i. http://satftp.soest.hawaii.edu/atlas/

Geary D.H., Brieske T.A. and Bemis B.E. (1992) The influence and interaction of temperature, salinity, and upwelling on the stable isotopic profiles of strombid gastropod shells. *Palaios* **7**(1), 77-85.

Goodbody Q.H. (1988) Devonian shelf systems on Melville island, Canadian High Arctic. In *Devonian of the World*, Vol. II (3 (ed., N.J. McMillan, A.F. Embry, D.J. Glass), pp. 29-51. Canadian Society of Petroleum Geologists.

Goodbody Q.H. (1994) Lower and Middle Paleozoic stratigraphy of Melville Island. *Geological Survey of Canada Bulletin* **450**, 23-104.

Goodbody Q.H. and Christie R.L. (1994) Summary of stratigraphy of Melville Island, Arctic Canada. *Geological Survey of Canada Bulletin* **450**, 13-22.

Graham D.W., Bender M.L., Williams D.F., Keigwin L.D. Jr. (1982) Strontium-calcium ratios in Cenozoic planktonic foraminifera. *Geochimica et Cosmochimica Acta* **46**, 1281-1292.

Grossman E.L. and Ku T.L. (1986) Oxygen and carbon fractionation in biogenic aragonite: Temperature effects. *Chemical Geology* **59**, 59-74.

Habermann D., Neuser R.D. and Richter D.K. (2000) Quantitative High Resolution Spectral Analysis of Mn^{2+} in Sedimentary Calcite. In *Cathodoluminescence in Geosciences* (ed. M. Pagel, V. Barbin, P. Blanc, and D. Ohnenstetter), pp. 331-358. Springer Verlag.

Harrison J.C., Goodbody Q.H., and Christie R.L. (1985) Stratigraphic and structural studies on Melville Island, District of Franklin. *Current Research, Part A, Geological Survey of Canada Paper* **85-1A**, 629-637.

Harrison J.C. (1994) A summary of the structural geology of Melville Island, Canadian Arctic Archipelago. *Geological Survey of Canada Bulletin* **450**, 257-283.

Hendry J.P. and Kalin, R.M. (1997) Are oxygen and carbon isotopes of mollusc shells reliable palaeosalinity indicators in marginal marine environments? A case study from the Middle Jurassic of England. *Journal of the Geological Society of London* **154**(2), 321-333.

Hendry J.P., Ditchfield P.W., and Marshall J.D. (1995) Two-stage neomorphism of Jurassic aragonite bivalves: Implications for early diagenesis. *Journal of Sedimentary Research* **A65**(1), 214-224.

Holmden C., Creaser R.A. and Muelenbachs K. (1997) Paleosalinities in ancient brackish water systems determined by $^{87}Sr/^{86}Sr$ ratios in carbonate fossils: A case study from the Western Canada Sedimentary Basin. *Geochimica et Cosmochimica Acta* **61**(10), 2105-2118.

Hudson J.D., Clements R.G., Riding J.B., Wakefield M.L., and Walton W. (1995) Jurassic Paleosalinities and Brackish-water Communities - A Case Study. *Palios* **10**, 392-407.

Ingram B. L. and DePaolo, D.J. (1993) A 4300 year strontium isotope record of estuarine paleosalinity in San Fransisco Bay, California. *Earth and Planetary Science Letters* **119**, 103-119.

Johnston P.A. and Goodbody Q.H. (1988) Middle Devonian bivalves from Melville Island, Arctic Canada. In *Devonian of the World*, Vol. 3 (ed., N.J. McMillan, A.F. Embry, D.J. Glass), pp. 337-346. Canadian Society of Petroleum Geologists.

Jones D.E. (1998) Isotopic determination of growth and longevity in fossil and modern invertebrates. *Isotope Paleobiology and Paleoecology*, 37-67.

Jones D.S., Thompson I. and Ambrose W.G. (1978) Age and growth rate determinations for the Atlantic surf clam *Spisula solidissima* based on internal growth lines in shell cross-sections. *Marine Biology* **47**(63-70).

Keith M. L. and Parker, R.H. (1965) Local variation of ^{13}C and ^{18}O content of mollusk shells and the relatively minor temperature effect in marginal marine environments. *Marine Geology* **3**, 115-129.

Krantz D.E., Williams D.F. and Jones D.S. (1987) Ecological and paleoenvironmental information using stable isotope profiles from living and fossil molluscs. *Palaeogeography, Palaeoclimatology, Palaeoecology* **58**, 249-266.

Kulp J.L., Turekian K., and Boyd D.W. (1952) Strontium content of limestones and fossils. *Bulletin of the Geological Society of America* **63**, 701-716.

Levitus S. and Boyer T. P. (1994) *World ocean atlas 1994, Volume 4: Temperature.* Washington, D.C. NOAA Atlas NESDIS, 117p.

Lowenstam H.A. (1961) Mineralogy, O^{18}/O^{16} ratios, and strontium and magnesium contents of Recent and fossil brachiopods and their bearing on the history of the oceans. *The Journal of Geology* **69**(3), 241-260.

Machel H. (1985) Cathodoluminescence in calcite and dolomite and its chemical interpretation. *Geoscience Canada* **12**, 139-147.

Machel H.G. (2000) Application of Cathodoluminescence to Carbonate Diagenesis. In *Cathodoluminescence in Geosciences* (ed. M. Pagel, V. Barbin, P. Blanc, and D. Ohnenstetter), pp. 271-302. Springer Verlag.

Maliva R.G. and Dickson J.A.D. (1992) The mechanism of skeletal aragonite neomorphism; evidence from neomorphosed mollusks from the upper Purbeck Formation (Late Jurassic-Early Cretaceous), southern England. *Sedimentary Geology* **76**(4), 221-232.

Maliva R.G. (1998) Skeletal aragonite neomorphism - quantitative modelling of a two-water diagenetic system. *Sedimentary Geology* **121**, 179-190.

Marshall D.J. (1988) *Cathodoluminescence of geological materials*. Unwin Hyman Ltd.

Martin G.D., Wilkinson B.H., and Lohmann K.C. (1986) The role of skeletal porosity in aragonite neomorphism - *Strombus* and *Montastrea* from the Pleistocene Key Largo Limestone, Florida. *Journal of Sedimentary Petrology* **56**(2), 194-203.

Mason R.A. (1987) Ion microprobe analysis of trace elements in calcite with an application to the cathodoluminescence zonation of limestone cements from the Lower Carboniferous of South Wales, UK. *Chemical Geology* **88**, 191-206.

Mason R.A. (1997) The influence of heating on cathodoluminescence emission from natural calcite. *Canadian Mineralogist* **35**, 723-733.

McCrea J.M. (1950) On the isotopic chemistry of carbonates and a paleotemperature scale. *Journal of Chemical Physics* **18**, 849-857.

Mook W.G. and Vogel J.C. (1967) Isotopic equilibrium between shells and their environment. *Science* **159**, 874-875.

Mook W.G. (1970) Paleotemperatures and chlorinities from stable carbon and oxygen isotopes in shell carbonate. *Palaeogeography, Palaeoclimatology, Palaeoecology* **9**, 245-263.

Nemec W. (1990) Deltas; remarks on terminology and classification. In *Coarse-grained deltas*, Vol. 10 (ed. A. Colella and D. B. Prior), pp. 3-12. Blackwell Scientific Publications.

Odum H.T. (1951) The stability of the world Sr cycle. *Science* **114**, 407-411.

Odum H.T. (1957) Biogeochemical deposition of strontium. *Publications of the Institute of Marine Science, University of Texas* **4**(2), 38-114.

O'Neil J.R., Clayton R.N. and Mayeda T.K. (1969) Oxygen isotope fractionation in divalent metal carbonates. *Journal of Chemical Physics* **51**, 5547-5558.

O'Neill B., Nguyen J.H., and Jeanloz R. (1993) Rapid computer analysis of X-ray diffraction films. *American Mineralogist* **78**, 1332-1335.

Pagel M., Barbin V., Blanc P., and Ohnenstetter D. (2000) Cathodoluminescence in Geosciences: An Introduction. In *Cathodoluminescence in Geosciences* (ed. M. Pagel, V. Barbin, P. Blanc and D. Ohnenstetter), pp. 1-22. Springer Verlag.

Palmer D.C. (1997) Digital analysis of X-ray films. *Mineralogical Magazine* **61**, 453-461.

Palmer M.R. and Edmond J.M. (1989) The strontium isotope budget of the modern ocean. *Earth and Planetary Science Letters* **92**, 11-26.

Presley B.J., Kolodny Y., Nissenbaum A., and Kaplan I.R. (1972) Early diagenesis in a reducing fjord, Saanich Inlet, British Columbia; II, Trace element distribution in interstitial water and sediment. *Geochimica et Cosmochimica Acta* **36**(10), 1073-1090.

Purton L.M.A., Shields G.A., Brasier M.D., and Grime G.W. (1999) Metabolism controls Sr/Ca ratios in fossil aragonitic mollusks. *Geology* **27**(12), 1083-1086.

Rosenthal Y. and Katz A. (1989) The applicability of trace elements in freshwater shells for paleogeochemical studies. *Chemical Geology* **78**, 65-76.

Scotese C. R. and McKerrow W. S. (1990) Revised World Maps and Introduction. In *Paleozoic Palaeogeography and Biogeography*, The Geological Society of London Memoir No. 12 (ed. C. R. Scotese and W. S. McKerrow), pp. 1-24.

Scotese C. R. (2000) Paleomap project. *http://www.scotese.com.*

Sandberg P. A. (1985) Nonskeletal aragonite and pCO_2 in the Phanerozoic and Proterozoic. In *The Carbon Cycle and Atmospheric CO_2: Natural Variations Archean to Present*, Vol. Monograph 32 (ed. E. T. Sundquist and W. S. Broecker), pp. 585-594. American Geophysisists Union.

Smith S.V., Buddemeier R.W., Redalje R.C., and Houck J.E. (1979) Strontium-calcium thermometry in coral skeletons. *Science* **204**(4391), 404-407.

Taylor J. D., Kennedy W.J. and Hall A. (1969) The shell structure and mineralogy of the Bivalvia. Introduction. Nuculacea - Trigonacea. *Bulletin of the British Museum (Natural History), Zoology Supplement* **no. 3**, 1-125.

Thompson T.G. and Chow T.J. (1955) The strontium, calcium ratio in carbonate secreting marine organisms. *Deep-Sea Research* **3**, 20-39.

Urey H.C., Epstein S., Lowenstam H.A. and McKinney C.R. (1951) Measurement of paleotemperatures and temperatures of the upper Cretaceous of England, Denmark, and the southeastern United States. *Geological Society of America Bulletin* **62**(4), 399-416.

Veizer J. (1977) Geochemistry of Lithographic Limestones and Dark marls from the Jurassic of southern Germany. *N. Jb. Geol. Palaont. Abh.* **153**(1), 129-146.

Veizer J., Ala D., Asmy K., Bruckschen P., Buhl D., Bruhn F., Carden G., Diener A., Ebneth S., Godderis Y., Jasper T., Korte C., Pawellek F., Podlaha O., and Strauss H. (1999) $^{87}Sr/^{86}Sr$, $\delta^{13}C$ and $\delta^{18}O$ evolution of Phanerozoic seawater. *Chemical Geology* **161**, 59-88.

Wilkinson B. H., Owen R. M., and Carroll A. R. (1985) Submarine hydrothermal weathering, global eustasy, and carbonate polymorphism in Phanerozoic marine oolites. *Journal of Sedimentary Petrology* **55**, 171-183.

Yurtsever Y. and Gat J.R. (1981) Atmospheric waters. In *Stable Isotope Hydrology, Deuterium and Oxygen-18 in the Water Cycle* (ed. J.R. Gat and R. Gonfiantini), pp. 103-142. International Atomic Energy Agency.

Ziegler P.A. (1988) Laurussia - The Old Red Continent. In *Devonian of the World*, Vol. I (ed. N.J. McMillan, A.F. Embry and D.J. Glass), pp. 15-48. Canadian Society of Petroleum Geologists.

Appendix I. $\delta^{18}O$ time series data for *Limoptera* sp. (U of A P904).

Distance (mm)	δ^{18}**0** (°/$_{oo}$ **PDB)**
0.0	-7.3
0.3	-7.1
0.6	-6.9
0.9	-7.1
1.2	-7.2
1.5	-7.7
1.8	-8.8
2.0	-9.2
2.3	-9.1
2.6	-8.7
2.9	-9.4
3.2	-9.4